Interactive Redox–pH Effects on Iron and Manganese Solubility in Soils of the Farafra Oasis, Egypt

Sahar. M. Ismail [1*]

ABSTRACT

Micronutrient deficiencies, particularly of iron (Fe) and manganese (Mn), are major constraints to crop productivity in calcareous soils of arid and semi-arid regions. The Farafra Oasis, Egypt, is characterized by coarse textures, moderate $CaCO_3$ content, low organic matter, and alkaline pH—conditions that limit Fe and Mn solubility despite large total reserves. This study aimed to elucidate the interactive effects of redox potential (Eh), pH, carbonate buffering, and soil physicochemical properties on the solubility and bioavailability of Fe and Mn under field and laboratory conditions. Seven representative soils, ranging from sand to clay, were characterized using XRD, XRF, and detailed chemical analyses. Seasonal field monitoring under sorghum cultivation assessed Eh, pH, moisture, O_2, CO_2, and DTPA-extractable Fe and Mn across irrigation cycles. Laboratory incubations of sandy and clay soils evaluated redox and pH buffering capacities under aerobic and anaerobic conditions. Results revealed that total Fe (14,800–20,200 mg kg^{-1}) and Mn (280–820 mg kg^{-1}) were poor predictors of plant availability, as DTPA-extractable fractions consistently remained below 0.03% of the total. Soil 1 (sand) exhibited the lowest DTPA-Fe (4.5 mg kg^{-1}) and Mn (3.0 mg kg^{-1}), whereas Soil 7 (clay, OM-rich) recorded the highest (6.5 and 6.2 mg kg^{-1}, respectively). Extractable Fe and Mn correlated negatively with pH, EC, and $CaCO_3$, and positively with OM, CEC, and moisture/CO_2 flux (R^2 = 0.93 for Fe; R^2 = 0.91 for Mn). Laboratory incubations confirmed that redox regime exerted stronger control on Eh than pH. These findings demonstrate that Fe and Mn availability depends not on total content but on dynamic interactions among alkalinity, salinity, redox buffering, and organic matter. Integrated strategies—organic amendments, Fe-EDDHA fertilization, foliar Mn supplementation, and optimized irrigation—are recommended to sustain crop productivity in reclaimed desert soils.

Key words: calcareous soils, redox potential, pH buffering, iron and manganese solubility, Farafra Oasis, micronutrient management.

INTRODUCTION

Agricultural productivity in arid and semi-arid regions is strongly constrained by declining soil fertility, climate-induced water stress, and pervasive micronutrient deficiencies, most notably of iron (Fe) and manganese (Mn). Both elements are indispensable for plant energy metabolism: Fe underpins chloroplast electron-transport (e.g. PSI Fe-S clusters, cytochromes, ferredoxin), while Mn is essential for the oxygen-evolving complex of Photosystem II (PSII) and for reactive-oxygen-species (ROS) detoxification (Alejandro *et al.,* 2020; Rai *et al.,* 2021 and Smythers *et al.,* 2023); imbalances rapidly manifest as photochemical impairment and chlorosis under field conditions. These constraints are amplified in calcareous desert soils, where alkaline pH and abundant carbonates suppress Fe and Mn solubility despite large total pools. In Farafra's newly reclaimed soils—high in $CaCO_3$ (≈25–34%) and alkaline (pH ~7.8–8.5) with very low organic matter—strong carbonate/pH buffering favors the formation of Fe(III) oxyhydroxides (e.g., goethite/hematite) and Mn(III/IV) oxides (e.g., birnessite), while the scarcity of organic ligands limits chelation/reduction; together these processes depress DTPA-extractable Fe and Mn and predispose crops to iron-chlorosis (Palansooriya *et al.,* 2020; Fadl *et al.,* 2022 and Yassin *et al.,* 2023). Micronutrient availability in such soils is controlled mainly by coupled redox–pH controls, mineralogy, and moisture dynamics. Under oxidized, alkaline conditions, Fe^{3+}/Mn^{4+} predominate and are poorly soluble; wetting events can generate transient anoxic microsites that lower Eh and mobilize Fe^{2+}/Mn^{2+}, but the magnitude and persistence of this effect depend on the soil's redox and pH buffering capacities, texture, carbonate content, and biological oxygen demand. Classic and contemporary work on dissimilatory Fe (III)/Mn (IV) reduction and on anoxic microsites underscores these mechanisms and their field-scale variability (Lovley, 1991; Lacroix *et al.,* 2023 and Sparks *et al.,* 2023). Over longer times, irrigation can exacerbate secondary salinization, which depresses microbial activity and further reduces micronutrient uptake—especially in alkaline, carbonate-buffered matrices—tightening the biogeochemical constraints on Fe/Mn nutrition (Abrol *et al.,* 1988; Grattan & Grieve, 1999 and Rietz & Haynes, 2003). Closing the management gap requires pairing robust diagnosis with interventions that function under high-pH, carbonate-rich conditions. Operationally, DTPA extraction remains the standard for estimating plant-available Fe/Mn in near-neutral to calcareous soils, while agronomic options include organic-matter

DOI: 10.21608/asejaiqjsae.2025.454333

[1] Soil Chemistry and Physics Department; Water Resources and Desert Soils Division; Desert Research Center; 1 El-Mathaf St., El-Matreia; Cairo; Egypt.

Received, August 20, 2025, Accepted, September 21, 2025.

additions to enhance buffering, stable Fe chelates (notably o,o-isomer of EDDHA) for soil/fertigation delivery at high pH, targeted foliar Mn where required, and irrigation scheduling that mitigates salt accumulation, while still accommodating short moisture pulses that generate transient anoxic microsites known to mobilize Fe^{2+}/Mn^{2+}(López-Rayo *et al.,* 2015). Accordingly, this study addresses that gap by investigating the Farafra soils using an integrated field–laboratory framework to (i) **Characterize** Fe- and Mn-bearing phases by XRD/XRF and chemical analyses, (ii) **Assess** the influence of redox and pH buffering capacities on Fe/Mn solubility under field and laboratory conditions, (iii) **Monitor** seasonal fluctuations in extractable $Fe^{2+}$and Mn^{2+}in relation to irrigation, moisture, and organic matter decomposition, (iv) **Evaluate** correlations between total and DTPA-extractable Fe/Mn and key soil properties (pH, OM, $CaCO_3$, CEC); and (v) **Propose** management strategies (organic amendments, Fe-EDDHA fertilization, foliar Mn supplementation, irrigation optimization) for enhancing micronutrient availability in calcareous arid soils.

MATERIALS AND METHODS

Study Area

The research was conducted in the Farafra Oasis, Western Desert, Egypt between 27°03′–27°30′ N and 27°58′–28°30′ E. The area is hyper-arid zone (<10 mm rainfall), with hot summers (>40 °C), cool winters, low humidity, and high evapotranspiration (El-Sherif *et al.,* 2018). Topographically, the area comprises flat plains interspersed with shallow depressions and sporadic calcareous outcrops, at elevations ranging from 60 to 120 meters above sea level. Soils are sandy to clayey, calcareous (up to 35% $CaCO_3$), alkaline (pH > 8), low in organic matter (<0.5%), and subject to salinization due to shallow groundwater, high evaporation rates and inefficient irrigation practices (Ismail *et al.,* 2016 and El-Sherif *et al.*, 2018).

Soil Sampling and Monitoring

Seven textural classes (sand, loamy sand, sandy loam, sandy clay loam, loam, silty clay, clay) were sampled (0–30 cm) in summer and winter using a stratified random design. Physicochemical properties measured included particle size, bulk density, porosity, saturated hydraulic conductivity (ks, pH, EC, OM, CEC, and $CaCO_3$. Redox potential (Eh) was measured with platinum electrodes corrected to the Standard Hydrogen Electrode (Fiedler *et al.,* 2007). Total and DTPA-extractable Fe and Mn were analyzed by AAS (Lindsay and Norvell, 1978). Mineralogical composition was identified by XRD and major oxides by XRF.

Seasonal field monitoring under sorghum cultivation assessed in *situ* Eh, pH, moisture (TDR), temperature, O_2 (soil oxygen probe), CO_2 flux by portable Infrared Gas Analyzer (IRGA), and groundwater depth. Measurements were made at four growth stages: pre-irrigation, 24h post-irrigation, mid-season, and post-harvest. Composite soil samples were collected for laboratory analysis of EC, OM, $CaCO_3$ (total and active), and CEC. Total Fe and Mn were determined by aqua regia digestion (HCL-HNO_3, 3:1 v/v), and DTPA-extractable Fe and Mn by AAS. Statistical analysis used two-way ANOVA, LSD test, Pearson correlation, and regression (Gomez and Gomez, 1984).

Laboratory Simulation of Redox–pH Effects

Two contrasting soils (sand and clay) were incubated under aerobic and anaerobic conditions to investigate the interactive effects of redox buffering capacity (RBC) and pH buffering capacity (pHBC) on the solubility and mobility of Fe and Mn. Two redox regimes were imposed by aeration or N_2 flushing (Patrick *et al.,* 1973). Target pH levels (5.5, 6.5, 7.5, and 8.5) were adjusted with HCl or NaOH (Ponnamperuma, 1972). All incubations were conducted in the dark at a constant temperature of 25 ± 2 ℃, Eh was monitored with Pt electrodes corrected to SHE (Reddy & Delaune, 2008 and Sander & Koschorreck, 2020). After 10 days, porewater was analyzed for soluble Fe^{2+} and Mn^{2+} and measured by AAS (Yu *et al.*, 2001).

Analytical Procedures

Soil pH, EC, texture, bulk density, porosity, OM, CEC, and $CaCO_3$ were determined following standard methods (Klute *et al.,* 1986). Total Fe and Mn were measured after nitric–perchloric digestion, and DTPA-extractable Fe/Mn following Lindsay and Norvell (1978). Mineralogy was determined by XRD, and major oxides by XRF (Cornell & Schwertmann, 2003 and Violante *et al.,* 2010) and validated using internal quality controls included blanks, duplicates, and spike recovery.

Statistical Analyses

Data were analyzed by one-way and two-way ANOVA, with LSD at $p \leq 0.05$. Normality and variance homogeneity were checked (Field, 2018 and Montgomery, 2017). Pearson's correlation coefficients (r), coefficients of determination (R^2), and multiple linear regression (MLR) analyses were applied to identify factors affecting Fe and Mn availability. Analyses were conducted with SPSS v26.0 and GraphPad Prism v9.0.

RESULTS AND DISCUSSION

1. Physicochemical and Mineralogical Variability Among Farafra Soils

The seven representative soils from the Farafra Oasis displayed marked spatial variability in their physicochemical and mineralogical properties, directly influencing Fe and Mn. Soil textures ranged from sandy (Soil 1) to clayey (Soil 7), with sand content decreasing from 90.3% to 30.0% and clay content increasing from 4.6% to 40.8% (Table 1 and Fig. 1). This gradient in texture was associated with a decrease in bulk density (from 1.62 to 1.40 g/cm³) and a corresponding increase in porosity (from 38.87% to 47.17%). Finer-textured soils also retained more water; Soil 6 exhibited the highest field capacity (41.5%) and available water content (18.5%), compared to sandy, Soil 1 (8.1% and 4.6%, respectively), (Table 2). However, this enhanced water retention was accompanied by a significant reduction in soil permeability, as saturated hydraulic conductivity (Ks) declined markedly from 15.6 cm/hr in Soil 1 to just 0.4 cm/hr in Soil 7 (Table 2). This pattern is consistent with previous studies demonstrating that clay minerals such as smectite and kaolinite increase water-holding capacity through capillary action and interlayer expansion, but concurrently restrict air flow and water movement through the soil matrix (Jien & Wang, 2019 and Klopp *et al.,* 2020). As soils became finer and more moisture-retentive, oxygen diffusion declined, leading to a drop in Eh from 270 mV in Soil 1 to 225 mV in Soil 7 (Table 3). These more reducing conditions likely promoted microbial reduction of Fe^{3+} and Mn^{4+} into their soluble divalent forms (Fe^{2+} and Mn^{2+}), thereby enhancing their bioavailability (Sharma *et al.,* 2017 and Totsche *et al.,* 2018).

Soil 7, in particular, exhibited the highest DTPA-extractable Fe (6.5 mg/kg) and Mn (6.2 mg/kg), highlighting the role of reductive dissolution in mobilizing micronutrients (Table 3). All soils were alkaline, with pH ranging from 7.80 to 8.40 (Table 3). Strong negative correlations were observed between pH ($r = –0.75^*$) and Eh ($r = –0.81^*$) with DTPA-extractable Fe, and between pH ($r = –0.96^{**}$) and Eh ($r = –0.97^{**}$) with DTPA-extractable Mn (Table 4 and Figs. 4A and B), indicating that both alkaline and more oxidizing conditions constrain micronutrient solubility. This occurs due to the precipitation of metal hydroxides or carbonates and the reduced dissociation of metal–organic complexes (Rajput *et al.,* 2023).

Table 1. One-way ANOVA of particle size distribution, bulk density, and porosity in surface layers (0–30 cm) of representative soils from the Farafra Oasis

Soil Type	Texture Class	Sand (%)	Silt (%)	Clay (%)	Bulk Density (g/cm³)	Porosity (%)
Soil 1	Sand	90.3	5.1	4.6	1.62	38.87
Soil 2	Loamy Sand	79.8	15.2	5.0	1.58	40.38
Soil 3	Sandy Loam	65.1	16.9	18.0	1.55	41.51
Soil 4	Sandy Clay Loam	55.4	20.1	24.5	1.52	42.64
Soil 5	Loam	45.3	40.0	14.7	1.48	44.15
Soil 6	Silty Clay	10.2	50.1	39.7	1.42	46.41
Soil 7	Clay	30.0	29.2	40.8	1.40	47.17
LSD (0.05)	**—**	**48.899**	**27.261**	**26.049**	**0.143**	**5.379**

Note: Values represent means of three replicates per composite soil sample (n = 3). Statistical differences were assessed using one-way ANOVA followed by LSD (Least Significant Difference) post-hoc tests at $p \leq 0.05$. Degrees of freedom: between groups = 6; within groups = 14.

Table 2. One-way ANOVA of saturated hydraulic conductivity and moisture retention characteristics in surface layers (0–30 cm) of representative soils from the Farafra Oasis

Soil Type	Saturated hydraulic conductivity (K_s), cm/hr	Water content at – 1500 kPa	Water content at – 33 kPa	Available water (AW, %)	Initial water content at Sampling (%)
Soil 1	15.6	3.5	8.1	4.6	6.2
Soil 2	13.2	3.3	10.0	6.7	7.3
Soil 3	3.6	11.1	20.5	9.4	8.4
Soil 4	1.8	15.4	27.7	12.3	10.5
Soil 5	3.5	9.7	23.5	13.8	11.5
Soil 6	0.6	23.0	41.5	18.5	12.1
Soil 7	0.4	24.1	39.3	15.2	14.0
LSD (0.05)	**10.881**	**14.785**	**22.770**	**8.570**	**4.912**

Note: Values represent means of three replicates per composite soil sample (n = 3). Statistical differences were assessed using one-way ANOVA followed by LSD (Least Significant Difference) post-hoc tests at $p \leq 0.05$. Degrees of freedom: between groups = 6; within groups = 14.

Table 3. One-way ANOVA of chemical and micronutrient characteristics (0–30 cm depth) in representative soils of the Farafra Oasis, with LSD post-hoc test (n = 3)

Soil Type	pH (1:2.5)	EC (1:5) (dS/m)	OM (%)	$CaCO_3$ (%)	CEC (cmol/kg)	Redox Potential (Eh, mV)	Total-Fe (mg/kg)	DTPA- Fe (mg/kg)	Total-Mn (mg/kg)	DTPA-Mn (mg/kg)
Soil 1	8.40	1.17	0.23	5.8	1.45	270	14,800	4.5	280	3.0
Soil 2	8.20	1.34	0.41	11.7	8.10	250	15,300	4.8	300	3.8
Soil 3	8.00	1.61	0.48	9.5	8.80	250	16,100	5.3	320	4.4
Soil 4	7.90	2.01	0.78	15.5	10.25	245	16,800	5.6	340	5.0
Soil 5	7.85	2.16	1.00	13.7	13.32	240	17,200	4.9	360	5.2
Soil 6	7.82	2.45	1.10	11.3	15.53	230	17,800	5.5	390	5.8
Soil 7	7.80	2.64	1.08	9.2	19.44	225	20,200	6.5	820	6.2
LSD (0.05)	**0.395**	**0.975**	**0.619**	**5.567**	**10.165**	**25.989**	**3149.63**	**1.157**	**329.56**	**1.965**

Note: Values represent the mean of three replicates (n = 3) per composite soil sample. Statistical differences between means were assessed using one-way ANOVA followed by the LSD (Least Significant Difference) post-hoc test at $p \leq 0.05$. Degrees of freedom (Df): between groups = 6; within groups = 14.

For example, Soil 1—having the highest pH (8.40) and Eh (270 mV)—recorded the lowest DTPA-Fe (4.5 mg/kg) and Mn (3.0 mg/kg), whereas Soil 7, with the lowest pH (7.80) and Eh (225 mV), showed the highest extractable Fe and Mn levels. Calcium carbonate ($CaCO_3$) contents ranged from 5.8% in Soil 1 to 15.5% in Soil 4 and were negatively correlated with DTPA-Fe ($r = –0.16$) and Mn ($r = –0.42$), suggesting that $CaCO_3$-rich soils immobilize Fe and Mn via co-precipitation and sorptive interactions with carbonate surfaces (Shakeria and Saffari, 2020). Notably, Soil 4, despite having a relatively fine texture, displayed only moderate DTPA-Fe and Mn levels—likely due to its high $CaCO_3$ content. XRD analysis confirmed that calcite and dolomite were dominant in calcareous soils (Table 5; Fig. 2A), while XRF spectra (Fig. 2B) indicated elevated CaO levels. Electrical conductivity (EC) varied from 1.17 to 2.64 dS/m, with higher values typically found in finer soils such as Soil 6. EC was negatively correlated with DTPA-Fe ($r = –0.81^*$) and Mn ($r = –0.99^{**}$), (Table 4), likely due to ionic competition and osmotic effects that hinder root uptake (Sharma *et al.*, 2022).

Table 4. Pearson correlation coefficients (r), coefficients of determination (R^2), and standardized multiple regression coefficients (RC) for soil factors influencing DTPA-extractable Fe and Mn in representative soils of the Farafra Oasis

Soil variable	r (Fe)	R^2 (Fe)	RC (Fe)	r (Mn)	R^2 (Mn)	RC (Mn)
pH	–0.75 *	0.555	–0.42	–0.96 **	0.927	–0.40
Electrical Conductivity (dS/m)	–0.81 *	0.658	–0.38	–0.99 **	0.977	–0.35
Organic Matter, (%)	+0.69	0.470	+0.35	+0.97 **	0.932	+0.31
Calcium carbonate (%)	–0.16	0.025	–0.33	–0.42	0.177	–0.30
Cation Exchange Capacity (cmol/kg)	+0.82 *	0.680	+0.24	+0.97 **	0.950	+0.20
Redox Potential (Eh, mV)	–0.81 *	0.652	+0.29	–0.97 **	0.945	+0.26
Texture	–0.82 *	0.668	–0.20	–0.99 **	0.980	–0.18
Available Water (%)	+0.67	0.454	+0.27	+0.95 **	0.904	+0.25
Moisture Content at Sampling (%)	+0.82 *	0.678	+0.30	+0.98 **	0.968	+0.28
Total Fe (mg/kg)	+0.91 **	0.823	+0.31	+0.93 **	0.874	—
Total Mn (mg/kg)	+0.87 **	0.750	—	+0.71	0.503	+0.28
Model R^2	**—**	**0.93**	**—**	**—**	**0.91**	—

Note: Pearson correlation coefficients (r), their corresponding coefficients of determination ($R^2 = r^2$), and standardized multiple regression coefficients (RC) for the relationships between selected soil properties and DTPA-extractable iron (Fe) and manganese (Mn) in representative soils of the Farafra Oasis. All significance levels are based on LSD at $p \leq 0.05$. Texture was treated as an ordinal variable (1 = sand, ……,7 = clay). Positive values indicate direct relationships; negative values indicate inverse relationships.

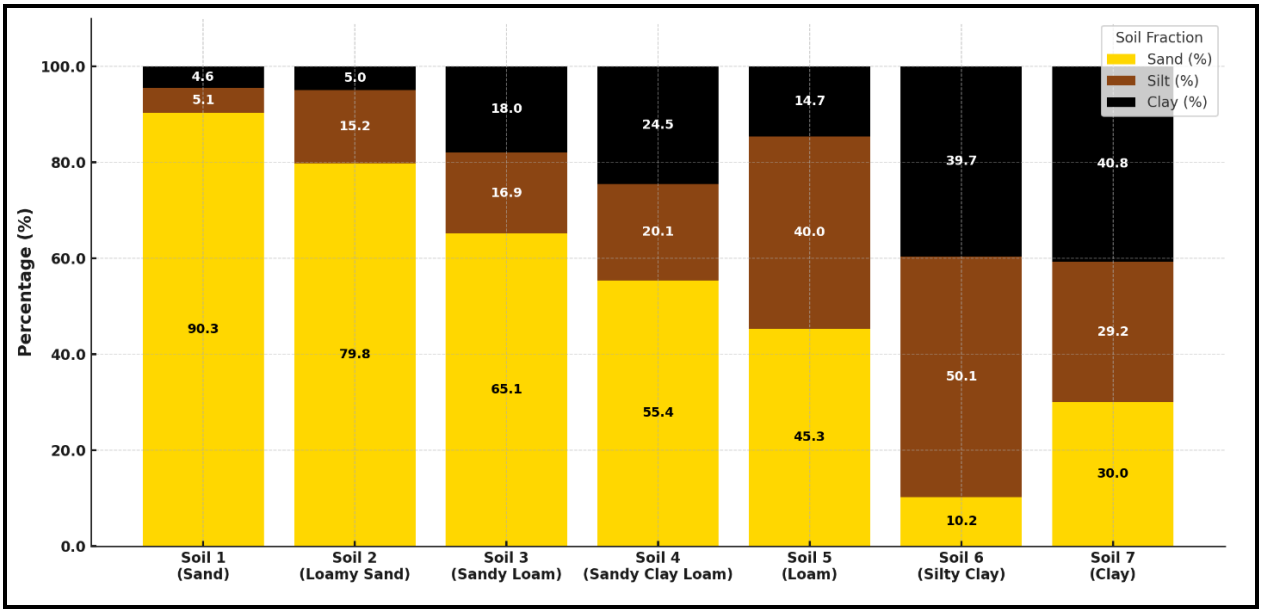

Figure 1. Particle size distribution (sand, silt, and clay fractions) in seven representative surface soils (0–30 cm depth) from the Farafra Oasis

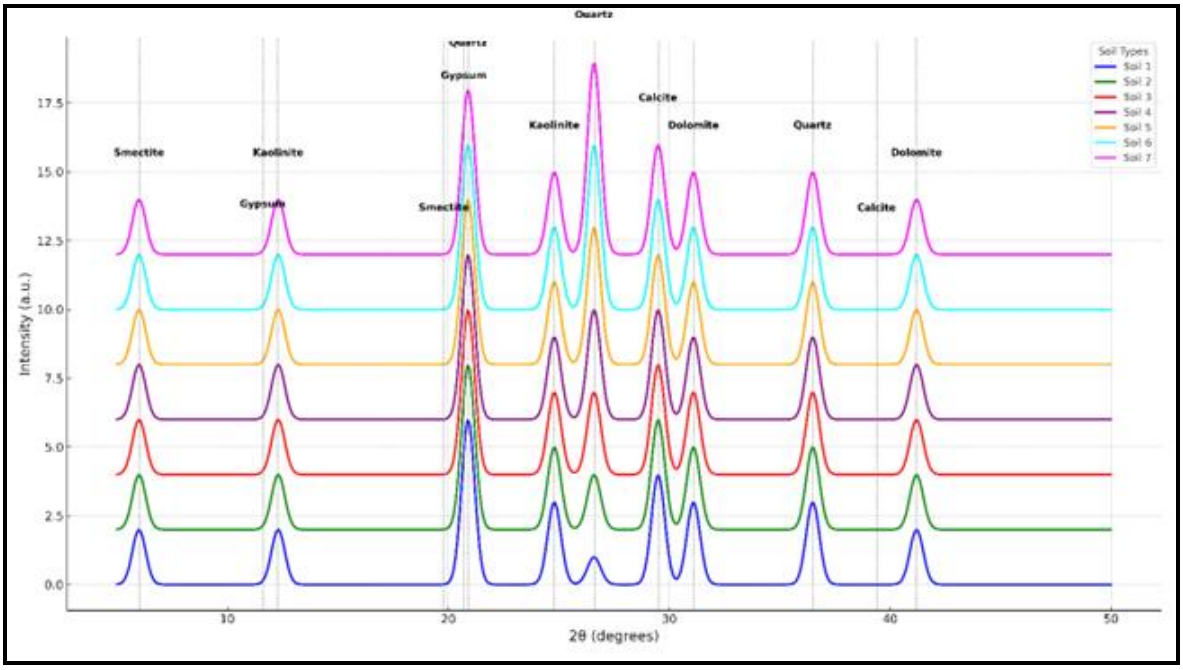

Figure 2A. X-ray diffraction (XRD) spectra of representative surface soils (0–30 cm) from the Farafra Oasis

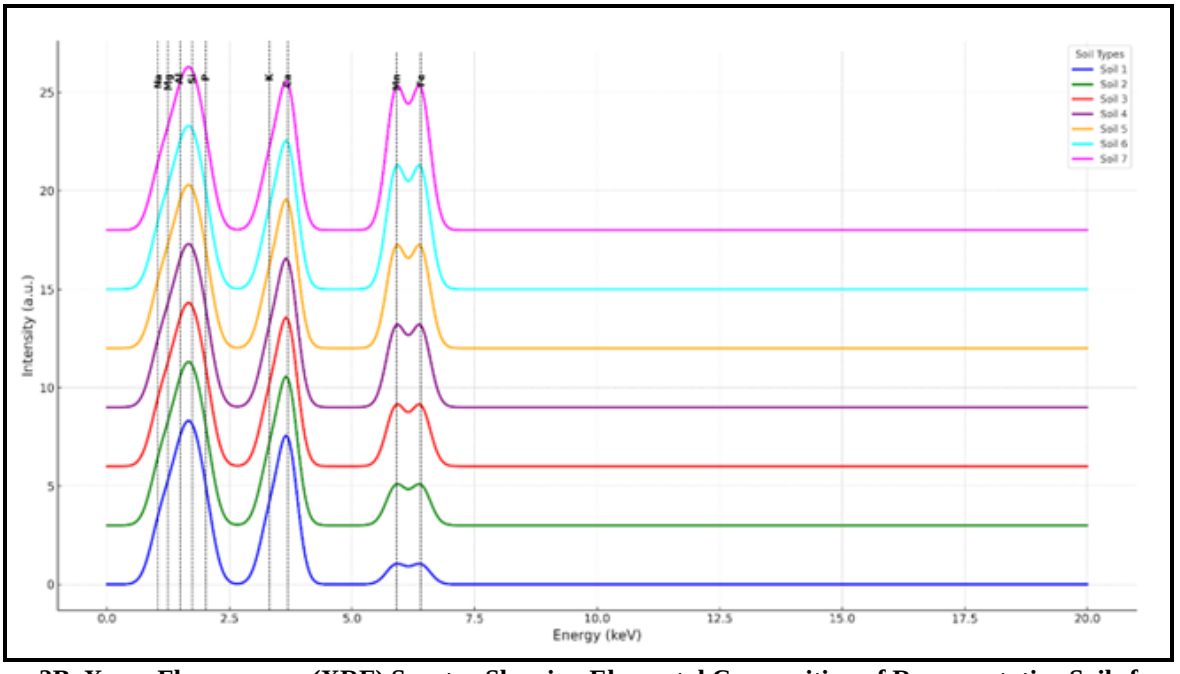

Figure 2B. X-ray Fluorescence (XRF) Spectra Showing Elemental Composition of Representative Soils from the Farafra Oasis

Table 5. Dominant mineralogical phases and major oxide composition of representative Farafra Oasis soils based on XRD and XRF analyses

Soil Type	Dominant Minerals (XRD)	Major Oxides (XRF)	Mineralogical Interpretation
Soil 1 (Sand)	Quartz (60%), Feldspar (25%), Minor Kaolinite	SiO_2 (70%), Al_2O_3 (15%), K_2O (5%)	Quartz-dominant, low-reactivity mineralogy; minimal nutrient retention
Soil 2 (Loamy Sand)	Quartz (50%), Calcite (15%), Kaolinite (10%)	SiO_2 (62%), CaO (12%), Al_2O_3 (10%)	Slightly more reactive than Soil 1; onset of carbonate buffering
Soil 3 (Sandy Loam)	Quartz (45%), Calcite (20%), Smectite (10%), Kaolinite	SiO_2 (58%), CaO (15%), Fe_2O_3 (6%)	Balanced composition; moderate CEC and improved buffering capacity
Soil 4 (Sandy Clay Loam)	Calcite (30%), Smectite (20%), Quartz (25%)	CaO (22%), SiO_2 (40%), Fe_2O_3 (8%)	Carbonate-rich with improved redox reactivity and water retention
Soil 5 (Loam, high $CaCO_3$)	Calcite (40%), Dolomite (20%), Quartz (15%)	CaO (30%), MgO (10%), SiO_2 (30%)	Strong carbonate buffering; potential Fe/Mn solubility constraints
Soil 6 (Silty Clay)	Calcite (35%), Smectite (25%), Minor Kaolinite	CaO (28%), SiO_2 (25%), Fe_2O_3 (10%), Na_2O (4%)	High carbonate content and clay reactivity; salinity may limit nutrient bioavailability
Soil 7 (Clay, high OM)	Smectite (40%), Kaolinite (30%), Minor Goethite	Fe_2O_3 (12%), Al_2O_3 (18%), SiO_2 (22%), OM present	High CEC and redox buffering; Fe/Mn oxides and OM support micronutrient availability

Note: Dominant crystalline minerals identified via X-ray diffraction (XRD) and corresponding major elemental oxides determined by X-ray fluorescence (XRF) are presented for seven representative surface soils (0–30 cm) from the farafra Oasis. Coarse-textured soils (Soils 1–3) are quartz-dominated with low reactivity, while finer soils (Soils 4–7) contain increasing proportions of calcite, smectite, and kaolinite, consistent with higher carbonate and clay content. Mineralogical interpretations are aligned with soil texture and chemical reactivity trends, particularly in relation to redox buffering, Fe/Mn availability, and cation exchange capacity. Oxide values are semi-quantitative and intended to reflect compositional trends rather than precise stoichiometry.

Organic matter (OM) contents, though generally low (0.23–1.10%), positively correlated with DTPA-Fe (r = +0.69*) and Mn (r = +0.97**), supporting the role of humic substances in micronutrient chelation and stabilization (de Santiago *et al.*, 2008). For instance, Soil 6, with the highest OM content (1.10%), exhibited relatively high levels of DTPA-extractable Fe and Mn despite elevated $CaCO_3$ levels. Cation exchange capacity (CEC) increased markedly from 1.45 to 19.44 cmol/kg (Table 3) and showed strong positive correlations with DTPA-Fe (r = +0.82*) and Mn (r = +0.97**). This reflects the impact of increased surface area and negative charge in clay- and OM-rich soils. However, the beneficial effect of high CEC was occasionally moderated by alkaline pH, high Eh, and $CaCO_3$ content, which limit the solubility and mobility of Fe and Mn even when adsorption capacity is high (Najafi-Ghiri *et al.*, 2010). Mineralogically, sandy soils (Soils 1–3) were dominated by quartz and feldspar, while finer-textured soils (Soils 4–7) were enriched with reactive mineral phases such as smectite, kaolinite, calcite, dolomite, and goethite (Table 5). These minerals are known to enhance Fe and Mn retention, redox buffering, and overall reactivity (Sparks, 2003 and Violante *et al.*, 2010). Elemental transitions observed in XRF spectra further confirmed a shift from Si and Al dominance in sandy soils to increased Ca, Fe, and Mn concentrations in clayey, calcareous soils—particularly in Soil 7.

2. Relationship Between Total and DTPA-Extractable Fe and Mn

Total Fe and Mn concentrations ranged from 14,800 to 20,200 mg/kg and 280 to 820 mg/kg, respectively (Table 3). However, the DTPA-extractable fractions of Fe and Mn were considerably lower—accounting for less than 0.03% of the total content Figure (Fig. 3). This large difference between total and DTPA-extractable

concentrations indicates that total Fe and Mn measurements alone cannot reliably predict the amounts actually available for plant uptake. In fact, total Fe and Mn concentrations showed weak or no correlation with key soil variables such as pH, OM, $CaCO_3$, and CEC (Table 4). In contrast, DTPA-extractable Fe and Mn were significantly influenced by chemical and physical soil characteristics (Figs. 4A, 4B) particularly pH, Eh, and EC (all negatively correlated), and OM and CEC (both positively correlated)—demonstrating that alkaline, saline, and more oxidizing conditions reduce micronutrient solubility, whereas higher organic matter and cation exchange capacity enhance it. For example, although Soil 6 had a relatively high total Fe concentration (17,800 mg/kg), it also exhibited elevated DTPA-Fe (5.5 mg/kg) due to its favorable combination of relatively low pH, low Eh, and high OM content, despite substantial $CaCO_3$ levels (15.53%).

More notably, Soil 7 showed the highest total Fe (20,200 mg/kg) and Mn (820 mg/kg) levels, along with the highest DTPA-extractable Fe (6.5 mg/kg) and Mn (6.2 mg/kg). These results are attributed to Soil 7's favorable combination of lower pH, higher OM (1.08%), elevated CEC (19.44 cmol/kg), fine texture, and low Eh (225 mV), which together promote the reductive dissolution of Fe^{3+} and Mn^{4+} oxides into plant-available Fe^{2+} and Mn^{2+}. This profile is further supported by its higher moisture retention and low permeability, which limit oxygen diffusion and maintain reducing conditions. These findings collectively illustrate that micronutrient availability in arid and semi-arid soils is affected by a complex interplay of chemical (pH, OM, $CaCO_3$, Eh), physical (texture, porosity), hydraulic (moisture retention, permeability), and mineralogical (clay content, reactive oxides) factors. As such, total Fe and Mn concentrations are insufficient proxies for estimating plant-available micronutrients. These results align with previous research in arid and semi-arid regions, which has shown that the availability of micronutrients is controlled more by their chemical forms, mineral binding, and surrounding soil microenvironments than by their total concentrations (Alloway, 2019; Yin *et al.*, 2020 and Wu *et al.*, 2021).

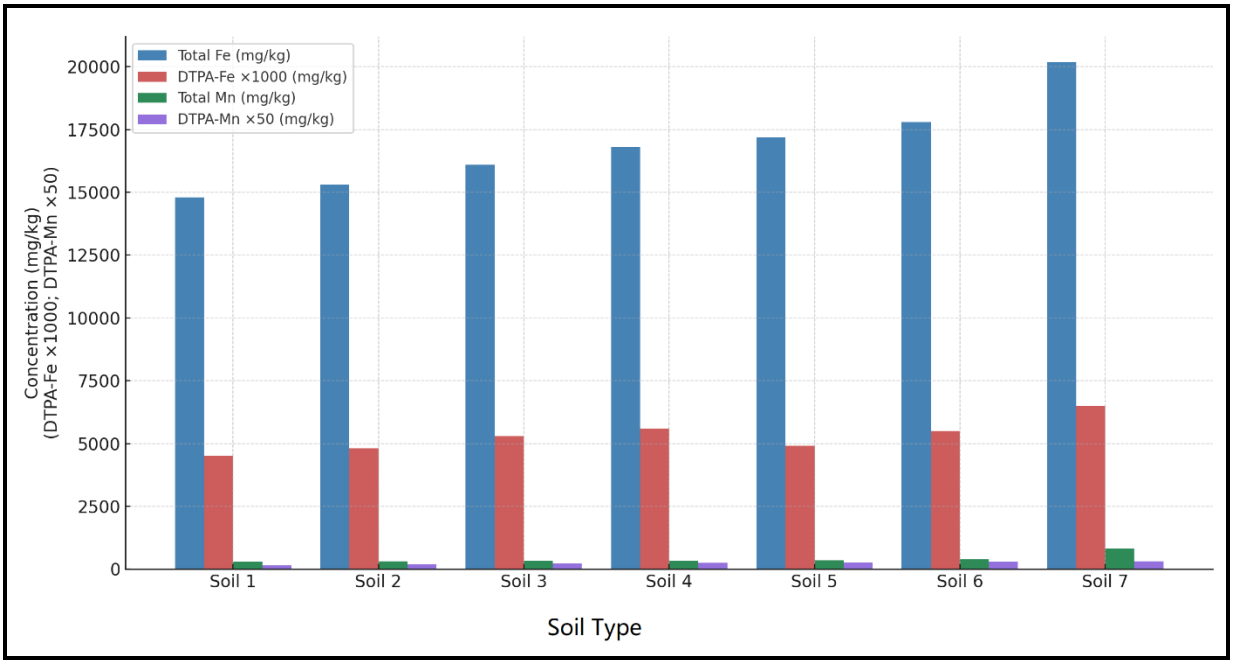

Figure 3. Comparison of total and DTPA-extractable iron (Fe) and manganese (Mn) concentrations in seven representative surface soils (0–30 cm) from the Farafra Oasis

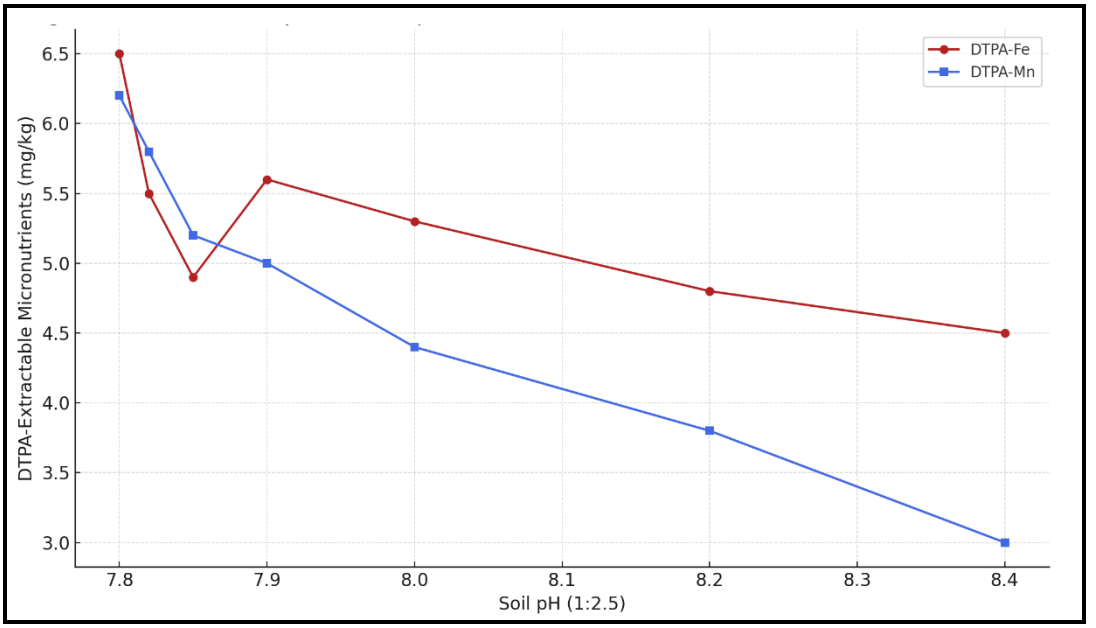

Figure 4A. Relationship between pH and DTPA-extractable iron (Fe) and manganese (Mn) in representative surface soils from the Farafra Oasis

.

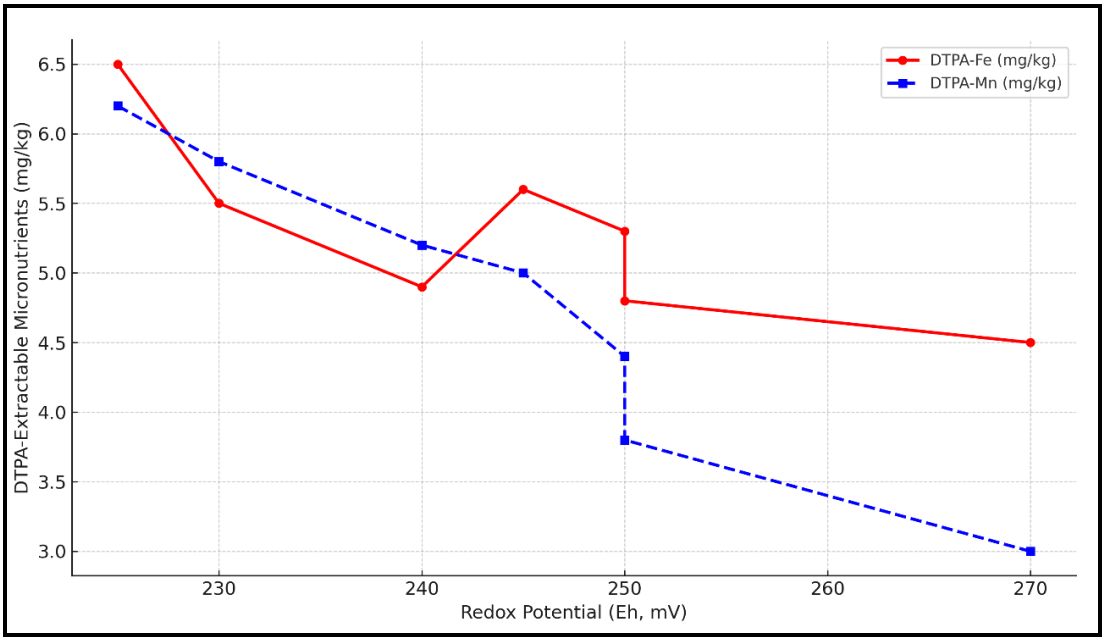

Figure 4B. Relationship between Redox Potential (Eh) and DTPA-Extractable Iron (Fe) and Manganese (Mn) in Representative surface Soils from the Farafra Oasis

3. **Seasonal redox–pH–moisture controls on Fe and Mn availability in Farafra Oasis soils**

Seasonal monitoring showed that irrigation cycles induced clear shifts in soil aeration and micronutrient solubility (Tables 6A, 6B; Figs. 5–7). After irrigation, soil moisture and CO_2 flux increased while O_2 declined, leading to lower Eh and temporary increases in DTPA-Fe and Mn. For the sand (Soil 1), moisture increased 6.2→10.0 %, CO_2 3.6→4.2 µmol m^{-2} s^{-1}, O_2 decreased 18→16 %, and DTPA-Fe and DTPA-Mn increased 4.5→4.9 and 3.0→3.4 mg kg^{-1}, respectively—illustrating significant main effects of soil and time and their interaction (soil × time) summarized in Table (6A) and Figs. (5–6). Mechanistically, irrigation stimulates microbial respiration, depresses O_2, and generates suboxic/anoxic microsites favoring Fe (III)→ Fe^{2+} and Mn (III/IV) → Mn^{2+} reduction. Such These effects were most evident in finer soils (e.g., Soils 6 and 7), where reduced aeration sustained higher extractable $Fe^{2+}$and Mn^{2+}(Evans *et al.,* 2021 and Hodges *et al.,* 2023). In coarse soils (Soil 1), oxidizing conditions re-established quickly due to high porosity, so post-irrigation increases in Fe and Mn were minimal and short-lived. By contrast, finer-textured soils retained moisture longer, generating suboxic conditions that favored reductive dissolution of Fe/Mn oxides and improved availability (Lakshani *et al.,* 2023 and Valdés-Abellán *et al.,* 2024). Correlation and regression analyses (Table 7) confirmed that DTPA-Fe and Mn correlated negatively with pH, EC, $CaCO_3$, O_2, and positively with OM, moisture, and CO_2 flux. Multiple-regression models, R^2 values were high (0.93 for Fe; 0.91 for Mn), indicating strong predictability. Eh shows only a moderate positive association with DTPA-Fe/Mn despite the clear O_2↓/CO_2↑ signature. Figs. (8A–8B and 9) summarize these interactions, showing that carbonate buffering maintains a low baseline of Fe/Mn solubility, while irrigation pulses cause short-term mobilization.

In Fig. (8A), high pH promotes poorly soluble Fe/Mn hydroxide/carbonate phases, depressing soluble (DTPA-extractable) fractions. Shifting toward more reducing conditions increases Fe^{2+}/Mn^{2+}, raising extractable Fe/Mn. The multivariate surface in Fig. (8B) embeds moisture, O_2, CO_2, EC, OM, and $CaCO_3$, predicting higher DTPA-Fe/Mn under wetter, low-O_2, high-CO_2 conditions and lower DTPA-Fe/Mn as pH/active $CaCO_3$. The conceptual path diagram (Fig. 9) summarizes this framework, with arrow signs and widths reflecting standardized regression coefficients (Table 7). These findings highlight that in Farafra's calcareous soils, Fe and Mn availability is constrained by high pH and salinity but can be transiently enhanced by irrigation-induced reducing conditions and organic matter inputs. However, improvements are temporary, and management practices (e.g., Fe-EDDHA fertilization, foliar Mn sprays, optimized irrigation) remain essential for correcting deficiencies (Rojas *et al.,* 2008; López-Rayo *et al.,* 2015; Dhaliwal *et al.,* 2023 and Zubieta *et al.,* 2025).

Table 6A. Two-way ANOVA of seasonal and soil type effects on some soil properties influencing DTPA-extractable Fe and Mn in representative soils of the Farafra Oasis"

Soil Type	Sampling Time	Eh (mV)	pH	Moisture Content, (%)	Soil Temp., (°C)	O_2, (%)	CO_2 Flux (µmol/m²/s)	DTPA-Fe (mg/kg)	DTPA-Mn (mg/kg)
Soil 1 (Sand)	Pre-irrigation	270	8.40	6.2	28	18	3.6	4.5	3.0
	24h post-irrigation	245	8.35	10.0	27	16	4.2	4.9	3.4
	Mid-season	260	8.38	8.5	30	17	4.0	4.7	3.2
	Post-harvest	255	8.42	7.0	29	18	3.8	4.6	3.1
Soil 2 (Loamy sand)	Pre-irrigation	250	8.20	7.3	27	19	2.8	4.8	3.8
	24h post-irrigation	230	8.12	11.5	26	15	4.0	5.2	4.1
	Mid-season	245	8.15	9.0	29	16	3.6	5.0	3.9
	Post-harvest	240	8.18	8.0	28	17	3.3	4.7	3.7
Soil 3 (Sandy loam)	Pre-irrigation	250	8.00	8.4	27	19	3.0	5.3	4.4
	24h post-irrigation	225	7.95	13.0	26	14	4.3	5.7	4.7
	Mid-season	240	7.98	10.5	29	16	3.8	5.5	4.5
	Post-harvest	235	8.02	9.3	28	17	3.5	5.2	4.3
Soil 4 (Sandy clay loam)	Pre-irrigation	245	7.90	10.5	26	18	3.2	5.6	5.0
	24h post-irrigation	220	7.80	15.2	25	13	4.5	6.0	5.4
	Mid-season	235	7.84	13.0	28	15	4.0	5.8	5.2
	Post-harvest	230	7.87	11.2	27	16	3.7	5.5	4.9
Soil 5 (Loam, high $CaCO_3$)	Pre-irrigation	240	7.85	11.5	26	17	3.3	4.9	5.2
	24h post-irrigation	215	7.75	17.2	25	12	4.3	5.3	5.6
	Mid-season	230	7.80	14.0	28	14	4.0	5.1	5.4
	Post-harvest	225	7.83	12.0	27	15	3.6	4.8	5.1
Soil 6 (Silty clay, high EC)	Pre-irrigation	230	7.82	12.1	25	16	3.5	5.5	5.8
	24h post-irrigation	205	7.67	18.5	24	11	4.4	6.0	6.1
	Mid-season	220	7.72	15.0	27	13	4.0	5.7	5.9
	Post-harvest	215	7.77	13.2	26	14	3.6	5.4	5.6
Soil 7 (Clay, high OM)	Pre-irrigation	225	7.80	14.0	25	15	3.6	6.5	6.2
	24h post-irrigation	200	7.65	20.5	24	10	4.6	7.0	6.7
	Mid-season	215	7.70	18.0	27	12	4.4	6.8	6.5
	Post-harvest	210	7.78	15.0	26	13	4.0	6.4	6.1
LSD (0.05)	-	**12.30**	**0.08**	**1.21**	**1.03**	**1.42**	**0.50**	**0.56**	**0.53**
Soil type effect	-	**	*	**	*	*	*	*	*
Sampling time effect	-	**	*	**	*	*	**	**	*
Interaction (Soil type × sampling time)	-	***	*	***	*	*	*	*	*

Note: Mean values of redox potential (Eh), pH, moisture content, soil temperature, oxygen concentration, CO_2 flux, and DTPA-extractable iron (Fe) and manganese (Mn) were measured across seven representative soil types during four seasonal sampling periods. Statistical differences among mean values for each variable were evaluated using a two-way ANOVA (factors: soil type × sampling time). The least significant difference (LSD) at the 0.05 probability level is provided for each variable. Asterisks (*, **, ***) denote statistical significance at $p \leq 0.05$, with more asterisks indicating stronger or more consistent significance across treatments.

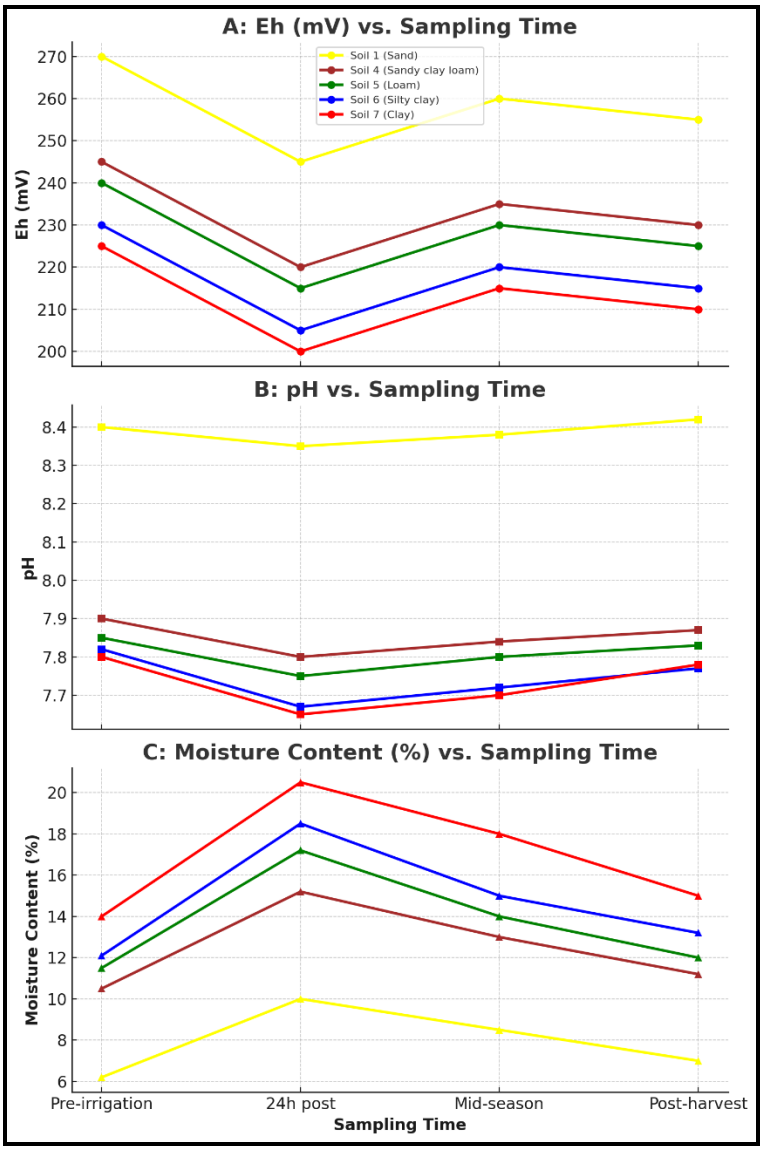

Figure 5. Seasonal variation of redox potential (Eh), pH, and volumetric moisture content in five representative soils of the Farafra Oasis

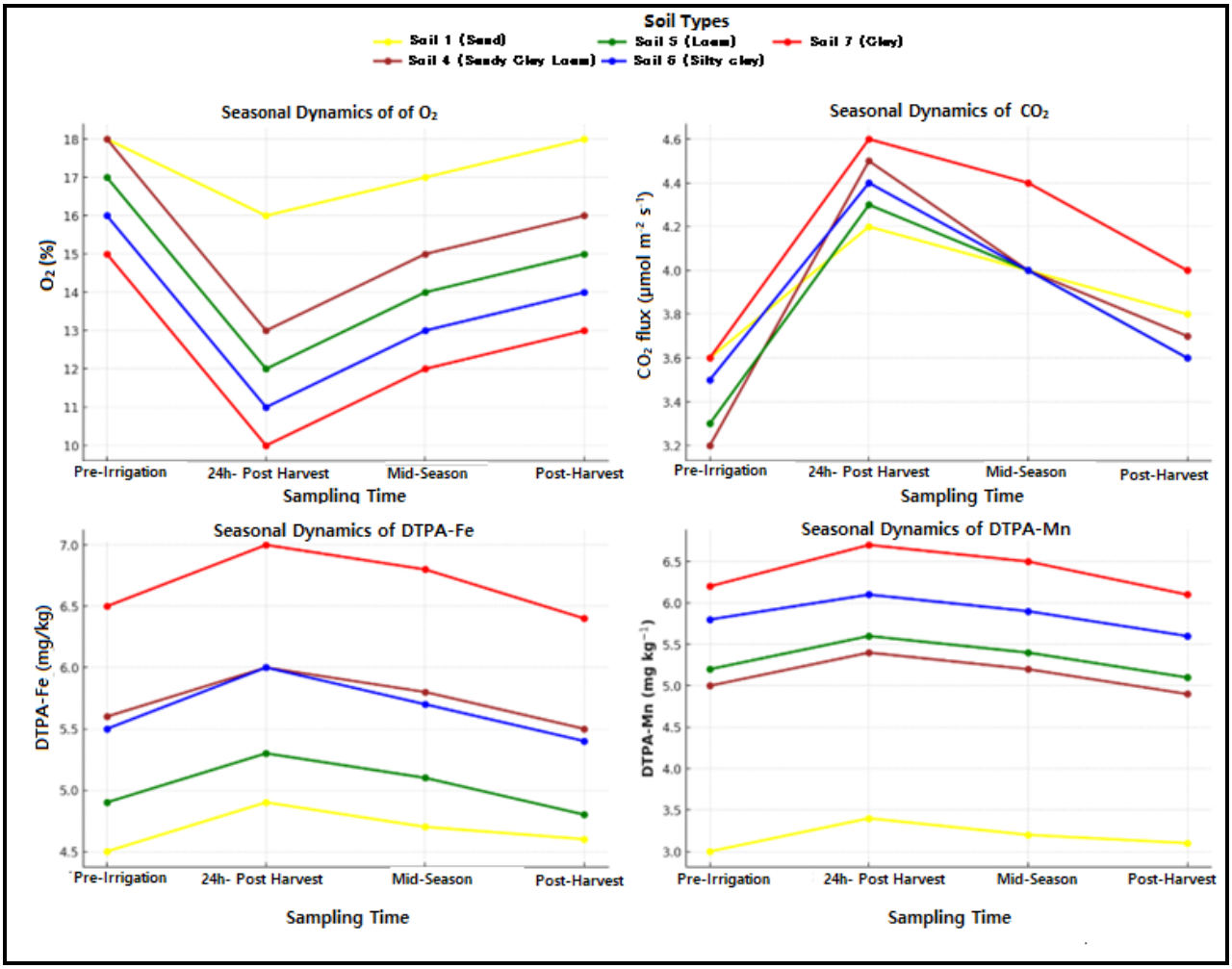

Figure 6. Seasonal dynamics of O_2, CO_2 flux, DTPA-Fe, and DTPA-Mn in five representative soils of the Farafra Oasis

Table 6B. Two-way ANOVA of seasonal and soil type effects on soil chemical properties related to Fe and Mn availability in representative soils of the Farafra Oasis

Soil Type	Sampling Time	EC (1:5), dS/m	OM (%)	$CaCO_3$ (%)	Active $CaCO_3$, (%)	CEC (cmol/kg)	Total Fe (mg/kg)	Total Mn (mg/kg)
Soil 1 (Sand)	Pre-Irrigation	1.17	0.23	5.8	1.40	1.45	14800	280
	24h post-irrigation	1.24	0.25	5.9	1.42	1.38		
	Mid-Season	1.35	0.21	6.0	1.45	1.42		
	Post-Harvest	1.29	0.22	5.7	1.40	1.38		
Soil 2 (Loamy Sand)	Pre-Irrigation	1.34	0.41	11.7	3.00	8.1	15300	300
	24h post-irrigation	1.48	0.45	11.9	3.05	8.3		
	Mid-Season	1.62	0.38	12.0	2.98	8.5		
	Post-Harvest	1.55	0.40	11.6	3.01	8.0		
Soil 3 (Sandy Loam)	Pre-Irrigation	1.61	0.48	9.5	2.50	8.8	16100	320
	24h post-irrigation	1.73	0.52	9.6	2.55	9.0		
	Mid-Season	1.85	0.43	9.7	2.47	9.2		
	Post-Harvest	1.76	0.45	9.4	2.51	8.7		
Soil 4 (Loam)	Pre-Irrigation	2.01	0.78	15.5	3.90	10.2	16800	340
	24h post-irrigation	2.18	0.83	15.7	3.95	10.5		
	Mid-Season	2.30	0.70	15.9	3.87	10.7		
	Post-Harvest	2.12	0.74	15.4	3.91	10.3		
Soil 5 (Silty Clay)	Pre-Irrigation	2.16	1.00	13.7	3.60	13.3	17200	360
	24h post-irrigation	2.35	1.08	13.9	3.65	13.6		
	Mid-Season	2.52	0.90	14.1	3.58	13.9		
	Post-Harvest	2.39	0.94	13.6	3.62	13.2		
Soil 6 (Clay Loam)	Pre-Irrigation	2.45	1.10	11.3	3.20	15.5	17800	390
	24h post-irrigation	2.68	1.13	11.5	3.25	15.8		
	Mid-Season	2.84	1.00	11.6	3.18	16.1		
	Post-Harvest	2.70	1.05	11.2	3.22	15.4		
Soil 7 (Clay)	Pre-Irrigation	2.64	1.08	9.2	2.90	19.4	20200	820
	24h post-irrigation	2.83	1.12	9.3	2.95	19.8		
	Mid-Season	2.92	0.96	9.5	2.87	20.1		
	Post-Harvest	2.79	1.00	9.1	2.91	19.2		
LSD (0.05)	-	**0.174**	**0.089**	**0.178**	**0.122**	**0.207**	—	—
Soil type effect	-	***	***	***	***	***	***	***
Sampling time effect	-	***	*	*	*	***	ns	ns
Interaction (Soil type × sampling time)	-	***	*	*	*	**	ns	ns

Note: Mean values of electrical conductivity (EC), organic matter (OM), total calcium carbonate ($CaCO_3$), active $CaCO_3$, cation exchange capacity (CEC), and total concentrations of iron (Fe) and manganese (Mn) were determined across seven representative soil types during four seasonal sampling periods. Total Fe and Mn values were considered stable and are presented as fixed values for each soil type. Statistical differences among means were assessed using a two-way ANOVA (factors: soil type × sampling time). The least significant difference (LSD) at the 0.05 probability level is provided for each variable. Asterisks (*, **, ***) indicate statistically significance at $p \leq 0.05$ with more asterisks denoting stronger or more consistent effects. "ns" indicates non-significance.

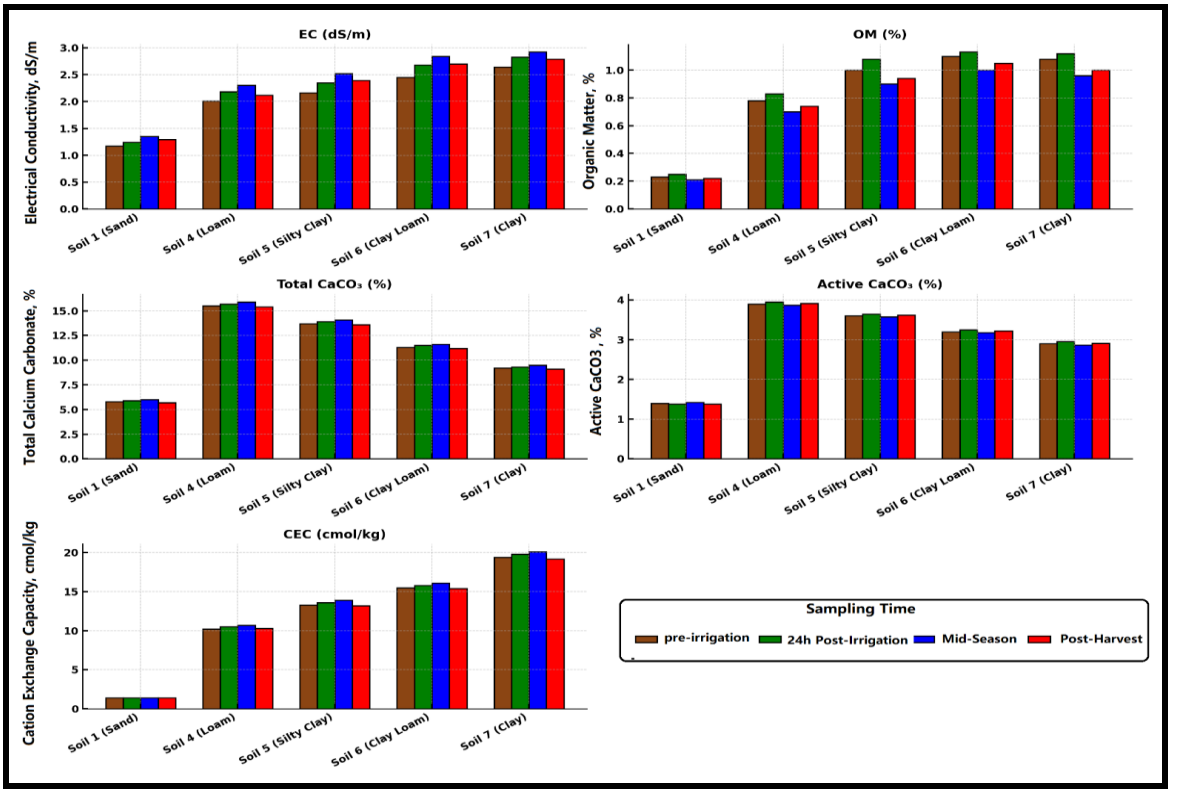

Figure 7. Seasonal dynamics of EC, OM, total $CaCO_3$, active $CaCO_3$, and CEC in five representative soils of the Farafra Oasis

Table 7. Pearson correlation coefficients (r), coefficients of determination (R^2), and standardized multiple regression coefficients (RC) for seasonal and soil variables influencing DTPA-extractable Fe and Mn in representative soils of the Farafra Oasis

Seasonal Variable	Fe (r)	R^2 (Fe)	RC (Fe)	r (Mn)	R^2 (Mn)	RC (Mn)	Fe (RC)
Redox Potential (Eh, mV)	+0.62*	0.384	+0.33	+0.58*	0.336	+0.29	+0.33
Soil pH	–0.72**	0.518	–0.81	–0.69**	0.476	–0.74	–0.81
Moisture Content (%)	+0.66*	0.436	+0.28	+0.63*	0.397	+0.25	+0.28
Soil Temperature (°C)	+0.40	0.160	+0.12	+0.35	0.123	+0.10	+0.12
Oxygen Concentration (%)	–0.60*	0.360	–0.27	–0.55*	0.303	–0.22	–0.27
CO_2 Flux (µmol/m²/s)	+0.70**	0.490	+0.36	+0.68**	0.462	+0.34	+0.36
Sampling Time (ordinal: 1–4)	–0.50	0.250	–0.20	–0.48	0.230	–0.18	–0.20
Electrical Conductivity (EC), (1:5), dS/m	–0.69**	0.476	–0.30	–0.65**	0.423	–0.28	–0.30
Organic Matter, (%)	+0.55*	0.303	+0.22	+0.53*	0.281	+0.20	+0.22
Calcium Carbonate ($CaCO_3$), (%)	–0.61*	0.372	–0.25	–0.58*	0.336	–0.22	–0.25
Active calcium carbonate (A-$CaCO_3$), %	–0.59*	0.348	–0.21	–0.56*	0.314	–0.19	–0.21
Cation Exchange Capacity (CEC), cmol/kg	+0.47	0.221	+0.18	+0.45	0.203	+0.16	+0.18
Total Fe, (mg/kg)	+0.62*	0.384	+0.27	+0.36	0.130	–	+0.27
Total Mn (mg/kg)	+0.40	0.160	–	+0.70**	0.490	+0.30	–
Model R^2	**-**	**0.93**	—	—	**0.91**	—	–

Note: Relationships between seasonal and soil variables and DTPA-extractable iron (Fe) and manganese (Mn) were assessed across 28 seasonal observations (7 soils × 4 sampling times) from the Farafra Oasis. Pearson correlation coefficients (*r*) represent simple linear associations, while coefficients of determination (R^2) indicate the proportion of variance explained by each variable individually ($R^2 = r^2$). Standardized multiple regression coefficients (RC) were derived from a full multiple linear regression model including all listed predictors. Model R^2 values for Fe (0.93) and Mn (0.91) represent the total variance in DTPA-extractable Fe and Mn explained by the respective full models. Asterisks (*) denote statistical significance at $p < 0.05$.

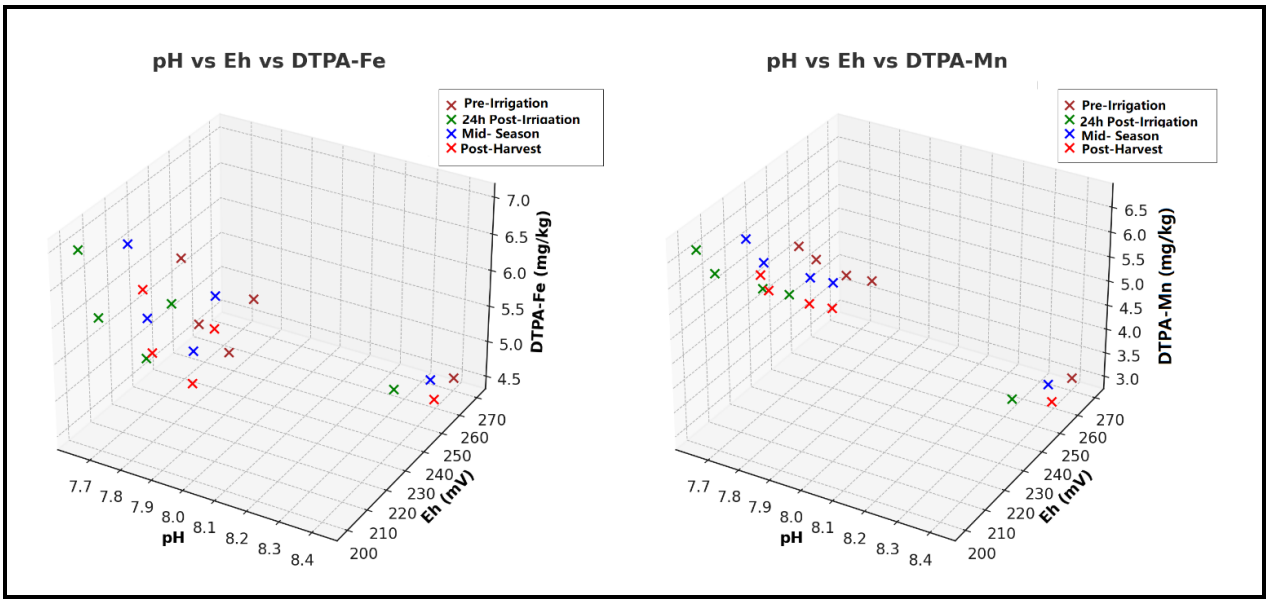

Figure 8A. 3D plots showing the combined effects of pH and Eh on Fe and Mn solubility

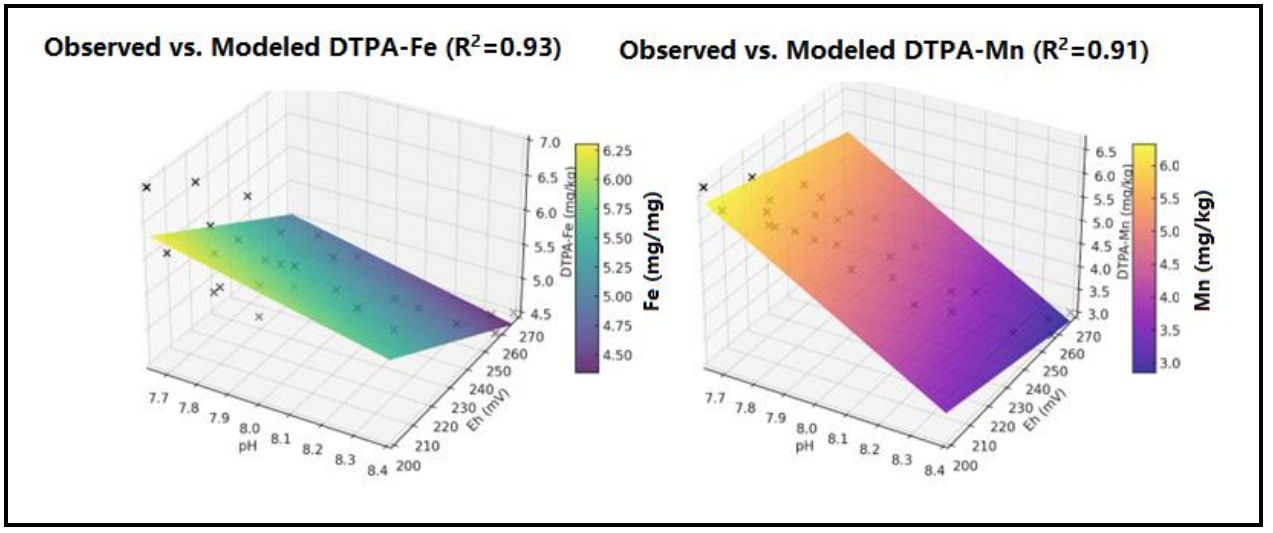

Figure 8B. 3D surface plots for Fe and Mn based on correlations from Table 7

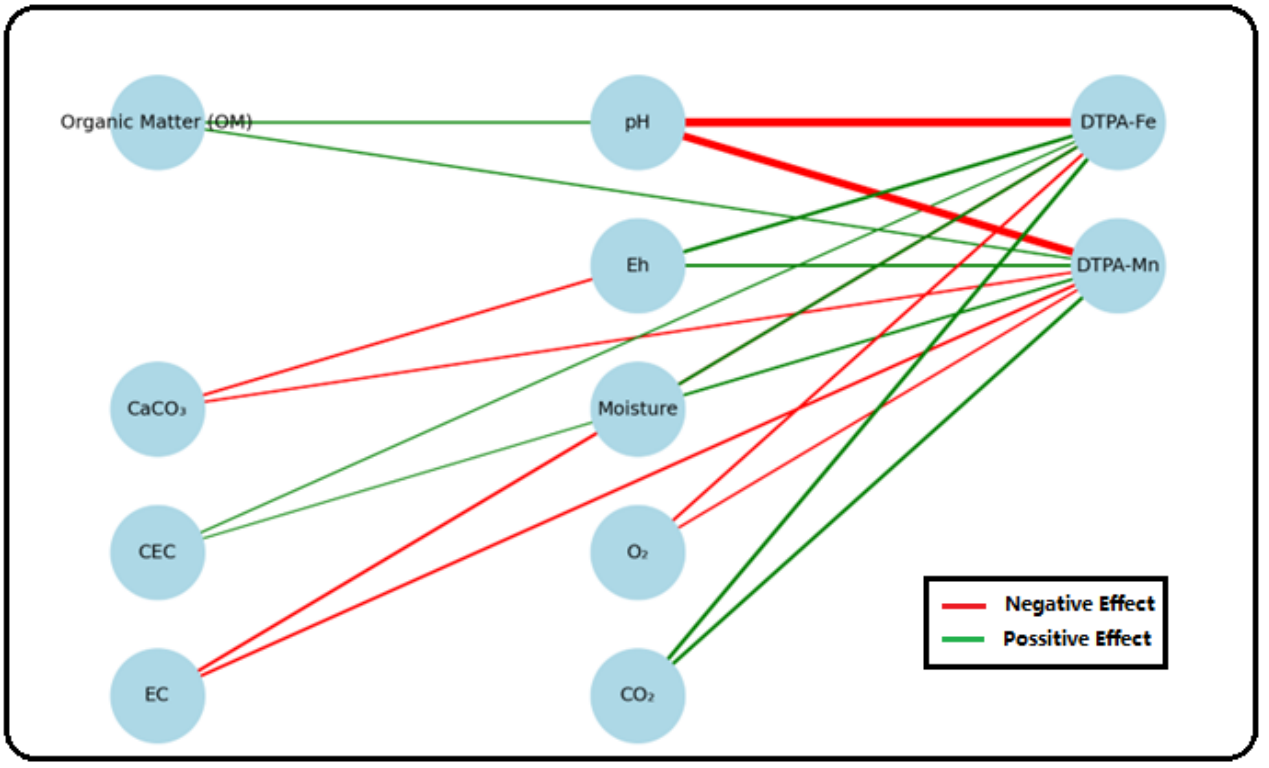

Figure (9). Conceptual path diagram based on Table 7, with arrow thickness proportional to standardized regression coefficients (RC) and colors indicating effect direction (green = positive, red = negative)

4. Redox potential (Eh) under aerobic and anaerobic conditions at different pH levels (laboratory incubation)

Incubation of sandy (Soil 1) and clayey (Soil 7) calcareous soils under aerobic vs. anaerobic conditions and four pH levels (5.5–8.5) showed that **redox regime dominated Eh more than pH**. In sand, aerobic Eh stayed high (~540–600 mV) while anaerobic Eh dropped sharply (~27–60 mV), creating conditions favorable for $Fe^{3+}$and Mn^{4+}reduction (Table 8; Fig. 10). In clay, Eh values were lower overall (~242–250 mV aerobic; 186–200 mV anaerobic), reflecting slower gas diffusion and higher OM/water retention (Table 9 and Fig. 10). These findings align with the dataset showing higher DTPA-Fe/Mn under anaerobiosis, stronger in sand than clay, and agree with published Fe/Mn redox thresholds (Lindsay & Norvell, 1978 and Palihakkara *et al.*, 2016).

Table 8. Daily Changes in pH and Redox Potential (Eh) of Soil 1 (Sand) under Aerobic and Anaerobic Conditions at Different Target pH Levels during a 10-Day Laboratory Incubation

	Aerobic		Anaerobic		Aerobic		Anaerobic		Aerobic		Anaerobic	
Day	pH (5.5)	Eh	pH (5.5)	Eh	pH (6.5)	Eh	pH (6.5)	Eh	pH (7.5)	Eh	pH (7.5)	Eh
1	5.52	540	5.50	30	6.50	560	6.50	40	7.50	580	7.48	50
2	5.49	535	5.48	28	6.48	555	6.46	38	7.52	575	7.50	48
3	5.50	538	5.47	27	6.50	557	6.47	37	7.49	578	7.47	46
4	5.51	540	5.49	29	6.53	559	6.48	39	7.48	579	7.49	47
5	5.53	542	5.50	31	6.51	561	6.49	40	7.51	580	7.50	48
6	5.52	541	5.49	30	6.52	560	6.50	39	7.50	579	7.48	47
7	5.50	539	5.48	28	6.50	558	6.48	37	7.52	577	7.49	46
8	5.49	538	5.47	27	6.48	557	6.46	36	7.50	575	7.47	45
9	5.51	540	5.49	29	6.51	559	6.49	39	7.48	578	7.48	47
10	5.52	541	5.50	30	6.52	560	6.50	40	7.50	580	7.50	48
LSD 0.05	**0.03**	**5**	**0.03**	**3**	**0.03**	**5**	**0.03**	**3**	**0.03**	**5**	**0.03**	**3**

Day	Aerobic		Anaerobic		Aerobic		Anaerobic	
	pH (8.5)	Eh	pH (8.5)	Eh	pH control	Eh control	pH control	Eh control
1	8.48	600	8.45	60	8.10	590	8.12	55
2	8.50	595	8.47	58	8.11	585	8.11	53
3	8.49	597	8.46	57	8.12	588	8.10	54
4	8.47	598	8.45	59	8.13	589	8.12	56
5	8.46	600	8.47	60	8.12	590	8.11	57
6	8.48	599	8.46	59	8.11	589	8.12	55
7	8.50	597	8.45	58	8.10	588	8.11	54
8	8.49	596	8.46	57	8.11	587	8.12	53
9	8.47	598	8.45	59	8.12	589	8.13	55
10	8.48	599	8.46	60	8.11	590	8.12	56
LSD 0.05	**0.05**	**5**	**0.05**	**3**	**0.05**	**5**	**0.05**	**3**

Note: Values represent treatment means (n = 3) for pH and Eh measured daily over the 10-day incubation period. Target pH levels were adjusted to 5.5, 6.5, 7.5, and 8.5, with an unadjusted control. $LSD_{0.05}$ denotes the least significant difference at the 5% probability level for comparisons within each parameter, calculated from the mean square error of a two-way ANOVA.

Table 9. Daily Changes in pH and Redox Potential (Eh) of Soil 7 (Clay) under Aerobic and Anaerobic Conditions at Different Target pH Levels during a 10-Day Incubation Period

	Aerobic		Anaerobic		Aerobic		Anaerobic		Aerobic		Anaerobic	
Day	pH (5.5)	Eh	pH (5.5)	Eh	pH (6.5)	Eh	pH (6.5)	Eh	pH (7.5)	Eh	pH (7.5)	Eh
1	5.52	247	5.50	200	6.51	246	6.49	196	7.50	244	7.48	191
2	5.49	246	5.48	198	6.49	248	6.46	194	7.52	247	7.50	190
3	5.50	249	5.47	196	6.50	250	6.47	193	7.49	249	7.47	188
4	5.51	248	5.49	197	6.53	251	6.48	195	7.48	246	7.49	189
5	5.53	250	5.50	199	6.51	249	6.49	196	7.51	248	7.50	190
6	5.52	249	5.49	198	6.52	247	6.50	195	7.50	245	7.48	188
7	5.50	246	5.48	197	6.50	246	6.48	193	7.52	244	7.49	187
8	5.49	245	5.47	196	6.48	245	6.46	192	7.50	243	7.47	186
9	5.51	247	5.49	198	6.51	247	6.49	194	7.48	246	7.48	188
10	5.52	248	5.50	199	6.52	248	6.50	196	7.50	246	7.50	189
LSD 0.05	**0.02**	**2.69**	**0.02**	**2.24**	**0.03**	**3.22**	**0.03**	**2.43**	**0.02**	**3.19**	**0.02**	**2.56**

Day	Aerobic		Anaerobic		Aerobic		Anaerobic	
	pH (8.5)	Eh	pH (8.5)	Eh	pH control	Eh control	pH control	Eh control
1	8.49	242	8.46	186	7.70	248	7.46	189
2	8.50	245	8.47	187	7.69	247	7.47	188
3	8.49	247	8.46	185	7.72	249	7.45	187
4	8.47	246	8.45	186	7.71	246	7.48	188
5	8.46	248	8.47	188	7.70	247	7.46	189
6	8.48	247	8.46	187	7.69	245	7.47	187
7	8.50	245	8.45	186	7.68	244	7.46	186
8	8.49	244	8.46	187	7.69	243	7.48	186
9	8.47	246	8.45	188	7.71	246	7.47	188
10	8.48	247	8.46	189	7.70	247	7.46	189
LSD 0.05	**0.02**	**3.00**	**0.01**	**2.04**	**0.02**	**3.09**	**0.02**	**1.98**

Note: Values represent treatment means (n = 3) for pH and Eh measured daily over the 10-day incubation period. Target pH levels were adjusted to 5.5, 6.5, 7.5, and 8.5, with an unadjusted control. $LSD_{0.05}$ denotes the least significant difference at the 5% probability level for comparisons within each parameter, calculated from the mean square error of a two-way ANOVA.

Redox buffer capacity (RBC) values were close to zero in both soils, indicating Eh stabilized quickly once O_2 status was imposed, with small positive/negative drifts that were not statistically significant (Tables 10–11; Fig. 11). In sand, small positive drifts appeared at pH 5.5-aerobic and the anaerobic control (+0.11 mV day^{-1}), with slight negatives at pH 7.5-anaerobic (–0.22) and pH 8.5-aerobic (–0.11). In clay, the range was slightly broader RBC ranges, peaking at pH 8.5-aerobic (+0.56) and dipping at pH 7.5-anaerobic (–0.22). All means shared the same $LSD_{0.05}$ group, confirming no significant treatment differences. The slightly higher RBC range in the clay suggests greater storage of electron acceptors (Fe/Mn oxides) and slower gas exchange, allowing marginal upward Eh drift under aeration, whereas small negatives under anaerobiosis reflect gradual oxidant depletion. Similar textural control studies on Eh behavior have been widely reported in waterlogged soils by Ponnamperuma (1972) and Reddy & DeLaune, (2008). Similarly, pH buffer capacity (pHBC) values were also near zero across treatments, confirming carbonate–bicarbonate buffering in calcareous soils (Dvořáčková et al., 2022). In sand, small positive drifts occurred at pH 7.5-anaerobic (0.0022 pH unit day^{-1}) and pH 8.5-anaerobic (0.0011); while in the clay, a positive shift appeared at pH 7.5-anaerobic (0.0022) and a slight negative at pH 8.5-aerobic (–0.0011). Again, treatments fell in the same statistical grouping (Tables 12–13 and Fig. 12). Collectively, the RBC and pHBC results demonstrate strong short-term buffering in both soils: with O_2 held constant, Eh rapidly stabilized at treatment-specific steady-state levels, and pH remained essentially unchanged over the 10-day incubation. DTPA-extractable Fe and Mn increased significantly under anaerobiosis at all pH levels, with maxima at pH 5.5 and minima at pH 8.5. In Soil 1, Fe rose from 4.65→7.92 mg/kg and Mn from 2.45→4.76 mg/kg (aerobic → anaerobic at pH 5.5), whereas at pH 8.5 Fe increased from 1.56 to 2.42 and Mn from 0.90 to 1.40 mg kg^{-1}; controls followed the same direction (Fe 1.32→1.84; Mn 0.80→1.10 mg kg^{-1}) (Table 14 and Figs. 13–14). Soil 7 showed the same trends (at pH 5.5 Fe rose 8.34→12.08 and Mn 5.20→8.10 mg kg^{-1}; at pH 8.5 Fe increased from 3.34→4.80 and Mn from 2.40→3.50 mg kg^{-1}) (Table 15 and Figs. 15–16). Relative increases were stronger in sand (~6× for Fe, ~5.95× for Mn) than clay (~4.2× and 4.05×). Regression confirmed Eh explained much of the variance in DTPA-Fe/Mn (Figs. 17–19). In parallel, pH–availability relations are generally inverse in these calcareous systems (Fig. 19). Near-zero RBC and pHBC (Tables 10–13) and their rankings (Tables 17–18) confirm day-to-day stability, reinforcing these associations. In short, **anaerobiosis mobilized Fe and Mn despite buffering**, with sand more responsive due to rapid aeration–deoxygenation cycles, while clay soils remained moderately reduced even under "aerobic" handling due to textural constraints (Lindsay & Norvell, 1978; Sparks, 2003 and Reddy & DeLaune, 2008).

Similarly, pH buffer capacity (pHBC) values were also near zero across treatments, confirming carbonate–bicarbonate buffering in calcareous soils (Dvořáčková et al., 2022). In sand, small positive drifts occurred at pH 7.5-anaerobic (0.0022 pH unit day^{-1}) and pH 8.5-anaerobic (0.0011); while in the clay, a positive shift appeared at pH 7.5-anaerobic (0.0022) and a slight negative at pH 8.5-aerobic (–0.0011). Again, treatments fell in the same statistical grouping (Tables 12–13 and Fig. 12). Collectively, the RBC and pHBC results demonstrate strong short-term buffering in both soils: with O_2 held constant, Eh rapidly stabilized at treatment-specific steady-state levels, and pH remained essentially unchanged over the 10-day incubation. DTPA-extractable Fe and Mn increased significantly

under anaerobiosis at all pH levels, with maxima at pH 5.5 and minima at pH 8.5. In Soil 1, Fe rose from 4.65→7.92 mg/kg and Mn from 2.45→4.76 mg/kg (aerobic → anaerobic at pH 5.5), whereas at pH 8.5 Fe increased from 1.56 to 2.42 and Mn from 0.90 to 1.40 mg kg^{-1}; controls followed the same direction (Fe 1.32→1.84; Mn 0.80→1.10 mg kg^{-1}) (Table 14 and Figs. 13–14). Soil 7 showed the same trends (at pH 5.5 Fe rose 8.34→12.08 and Mn 5.20→8.10 mg kg^{-1}; at pH 8.5 Fe increased from 3.34→4.80 and Mn from 2.40→3.50 mg kg^{-1}) (Table 15 and Figs. 15–16). Relative increases were stronger in sand (~6× for Fe, ~5.95× for Mn) than clay (~4.2× and 4.05×), (Table 16). Regression confirmed Eh explained much of the variance in DTPA-Fe/Mn (Figs. 17–19).In parallel, pH–availability relations are generally inverse in these calcareous systems (Fig. 19). Near-zero RBC and pHBC (Tables 10–13) and their rankings (Tables 17–18) confirm day-to-day stability, reinforcing these associations. In short, **anaerobiosis mobilized Fe and Mn despite buffering**, with sand more responsive due to rapid aeration–deoxygenation cycles, while clay soils remained moderately reduced even under "aerobic" handling due to textural constraints (Reddy & DeLaune, 2008; Lindsay & Norvell, 1978; and Sparks, 2023).

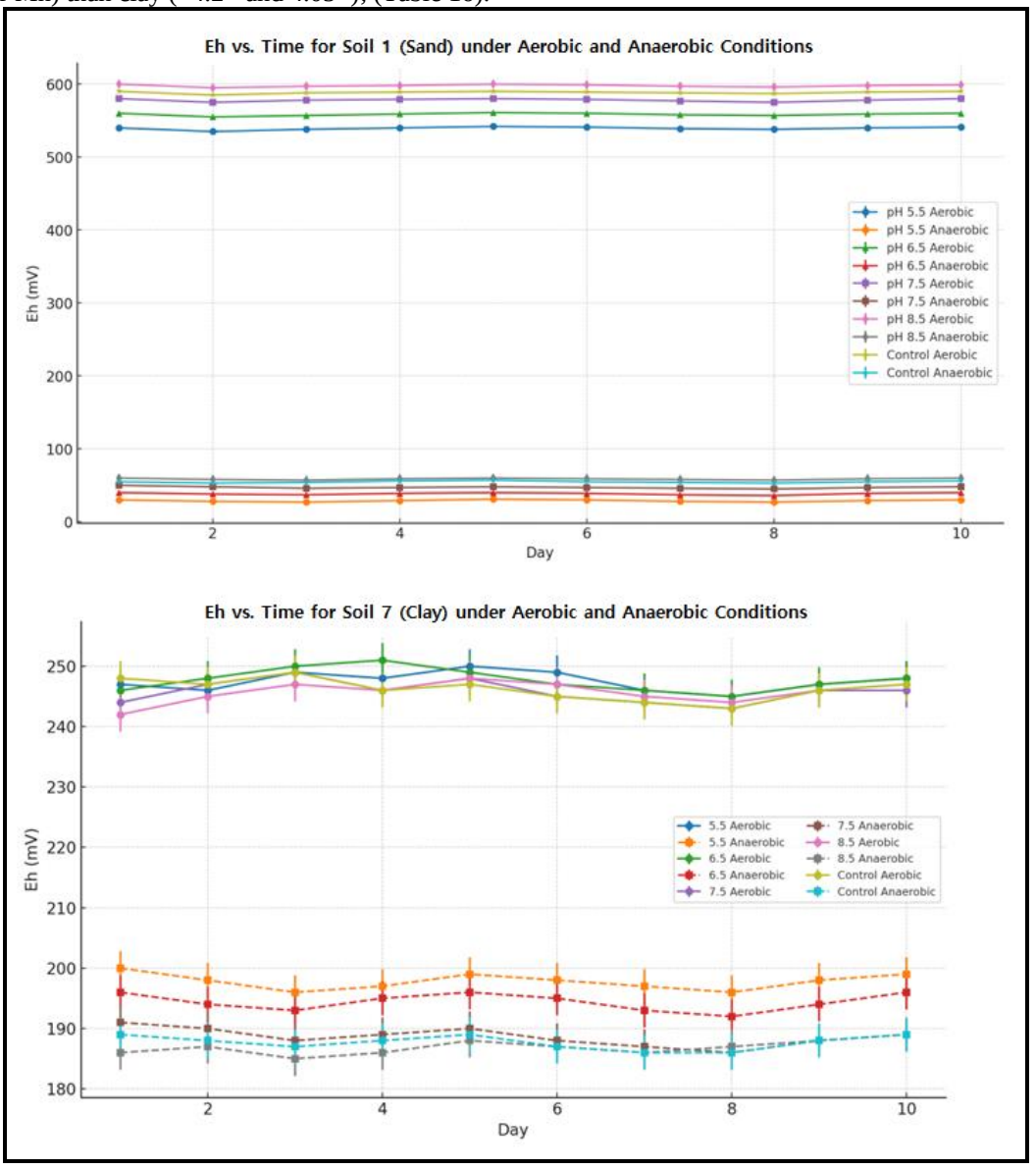

Figure 10.Changes in redox potential (Eh) during a 10-day incubation of Soils 1 (Sand) and 7 (Clay) under aerobic and anaerobic conditions

Table 10. Redox Buffer Capacity (RBC) of Soil 1 (Sand) under Aerobic and Anaerobic Conditions at Different Target pH Levels during a 10-Day Laboratory Incubation.

Treatment	RBC (mV/day)	LSD (0.05)	Statistical Group
pH 5.5 Aerobic	0.11	0.95	a
pH 5.5 Anaerobic	0.00	0.95	a
pH 6.5 Aerobic	0.00	0.95	a
pH 6.5 Anaerobic	0.00	0.95	a
pH 7.5 Aerobic	0.00	0.95	a
pH 7.5 Anaerobic	-0.22	0.95	a
pH 8.5 Aerobic	-0.11	0.95	a
pH 8.5 Anaerobic	0.00	0.95	a
pH Control Aerobic	0.00	0.95	a
pH Control Anaerobic	0.11	0.95	a

Note: RBC values are expressed as the rate of change in redox potential (mV day^{-1}) calculated over the 10-day incubation period. $LSD_{0.05}$ denotes the least significant difference at the 5% probability level for comparisons within each parameter, calculated from the mean square error of a two-way ANOVA. Means followed by the same letter are not significantly different according to the LSD test.

Table 11. Redox Buffer Capacity (RBC) of Soil 7 (Clay) under Aerobic and Anaerobic Conditions at Different Target pH Levels during a 10-Day Laboratory Incubation.

Treatment	RBC (mV/day)	LSD (mV)	Statistical Group
pH 5.5 Aerobic	0.11	0.51	a
pH 5.5 Anaerobic	-0.11	0.51	a
pH 6.5 Aerobic	0.22	0.61	a
pH 6.5 Anaerobic	0.00	0.61	a
pH 7.5 Aerobic	0.22	0.61	a
pH 7.5 Anaerobic	-0.22	0.61	a
pH 8.5 Aerobic	0.56	0.57	a
pH 8.5 Anaerobic	0.33	0.57	a
pH Control Aerobic	-0.11	0.59	a
pH Control Anaerobic	0.00	0.59	a

Note: RBC values are expressed as the rate of change in redox potential (mV day^{-1}) calculated over the 10-day incubation period. $LSD_{0.05}$ denotes the least significant difference at the 5% probability level for comparisons within each parameter, calculated from the mean square error of a two-way ANOVA. Means followed by the same letter are not significantly different according to the LSD test.

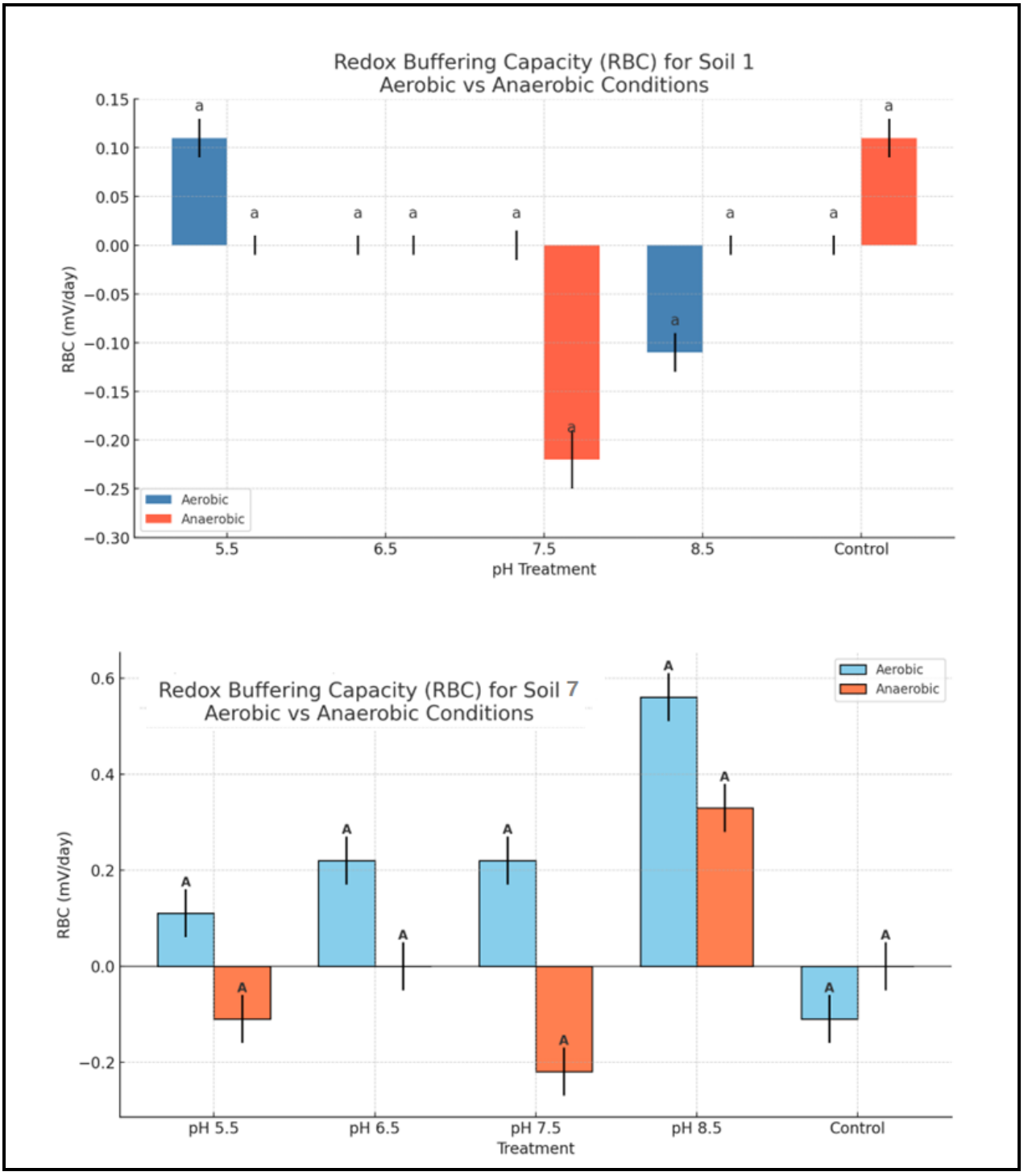

Figure 11. Redox Buffer Capacity (RBC) of Soil 1 (Sand) and Soil 7 (Clay) under Aerobic and Anaerobic Conditions at Different Target pH Levels during a 10-Day Laboratory Incubation

Table 12.'pH Buffer Capacity (pHBC) of Soil 1 (Sand) under Aerobic and Anaerobic Conditions at Different Target pH Levels during a 10-Day Laboratory Incubation

Treatment	pHBC (pH unit/day)	LSD (0.05)	Statistical Group
pH 5.5 Aerobic	0.0000	0.003	a
pH 5.5 Anaerobic	0.0000	0.003	a
pH 6.5 Aerobic	0.0000	0.003	a
pH 6.5 Anaerobic	0.0000	0.003	a
pH 7.5 Aerobic	0.0000	0.003	a
pH 7.5 Anaerobic	0.0022	0.003	a
pH 8.5 Aerobic	0.0000	0.005	a
pH 8.5 Anaerobic	0.0011	0.005	a
pH Control Aerobic	0.0011	0.005	a
pH Control Anaerobic	0.0000	0.005	a

Note: pHBC values are expressed as pH units per day, calculated over the 10-day incubation period. $LSD_{0.05}$ denotes the least significant difference at the 5% probability level for comparisons within each parameter, derived from the pH LSD values in Table 8 and scaled to a 10-day incubation.

Table 13. pH Buffer Capacity (pHBC) of Soil 7 (Clay) under Aerobic and Anaerobic Conditions at Different Target pH Levels during a 10-Day Laboratory Incubation

Treatment	pHBC (pH unit/day)	LSD (0.05)	Statistical Group
pH 5.5 Aerobic	0.0000	0.002	a
pH 5.5 Anaerobic	0.0000	0.002	a
pH 6.5 Aerobic	0.0011	0.003	a
pH 6.5 Anaerobic	0.0011	0.003	a
pH 7.5 Aerobic	0.0000	0.002	a
pH 7.5 Anaerobic	0.0022	0.002	a
pH 8.5 Aerobic	-0.0011	0.002	a
pH 8.5 Anaerobic	0.0000	0.001	a
pH Control Aerobic	0.0000	0.002	a
pH Control Anaerobic	0.0000	0.002	a

Note: pHBC values are expressed as pH units per day, calculated over the 10-day incubation period. $LSD_{0.05}$ denotes the least significant difference at the 5% probability level for comparisons within each parameter, derived from the pH LSD values in Table 9 and scaled to a 10-day incubation.

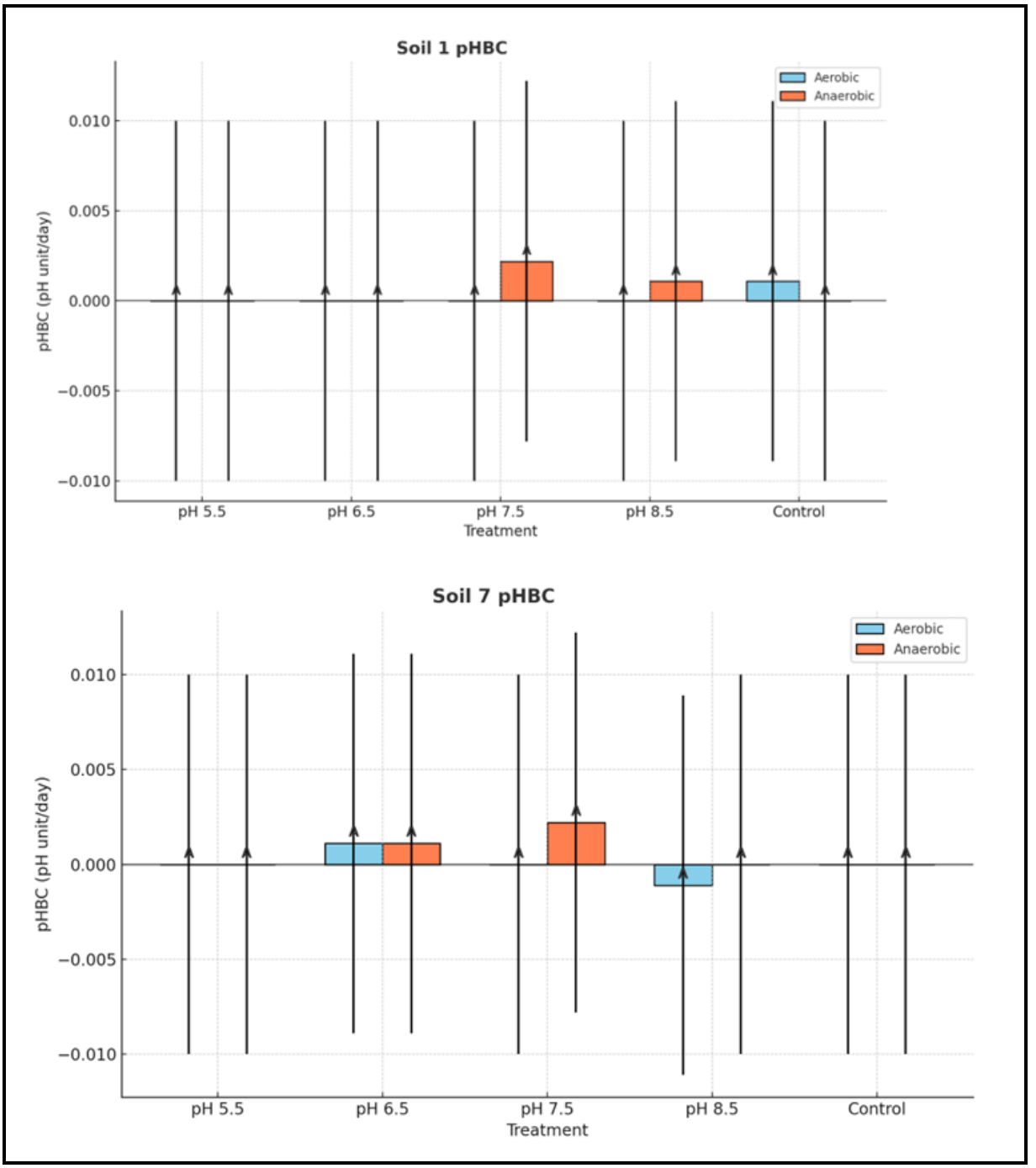

Figure 12. pH Buffer Capacity (pHBC) of Soil 1 (Sand) and Soil 7 (Clay) under Aerobic and Anaerobic Conditions at Different Target pH Levels during a 10-Day Laboratory Incubation

Table 14. DTPA-Extractable Iron (Fe) and Manganese (Mn) in Soil 1 (Sand) under Aerobic and Anaerobic Conditions at Different Target pH Levels during a 10-Day Laboratory Incubation

Treatment	Fe Mean ± SE	Mn Mean ± SE	Fe $LSD_{0\text{-}05}$	Mn $LSD_{0\text{-}05}$
pH 5.5 Aerobic	4.65 ± 0.010	2.45 ± 0.010	0.030	0.030
pH 5.5 Anaerobic	7.92 ± 0.010	4.76 ± 0.010	0.030	0.030
pH 6.5 Aerobic	3.52 ± 0.010	1.88 ± 0.010	0.030	0.030
pH 6.5 Anaerobic	6.04 ± 0.010	3.46 ± 0.010	0.030	0.030
pH 7.5 Aerobic	2.41 ± 0.005	1.30 ± 0.005	0.015	0.015
pH 7.5 Anaerobic	3.85 ± 0.005	2.20 ± 0.005	0.015	0.015
pH 8.5 Aerobic	1.56 ± 0.005	0.90 ± 0.005	0.015	0.015
pH 8.5 Anaerobic	2.42 ± 0.005	1.40 ± 0.005	0.015	0.015
Control Aerobic	1.32 ± 0.005	0.80 ± 0.005	0.015	0.015
Control Anaerobic	1.84 ± 0.005	1.10 ± 0.005	0.015	0.015

Note: Values represent means ± standard error (SE) of DTPA-extractable Fe and Mn concentrations (mg·kg⁻¹) measured over the 10-day incubation period (n = 3). $LSD_{0.05}$ denotes the least significant difference at the 5% probability level for comparisons within each parameter, calculated from the standard errors and sample size.

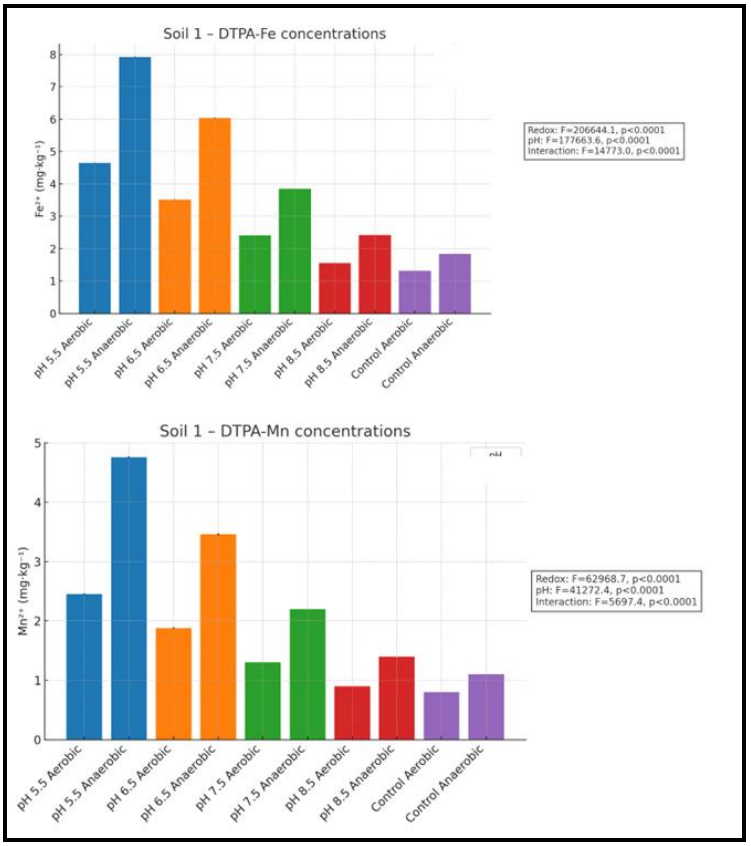

Figure 13. DTPA-Extractable Iron (Fe) and Manganese (Mn) in Soil 1 (Sand) under Aerobic and Anaerobic Conditions at Different Target pH Levels during a 10-Day Laboratory Incubation

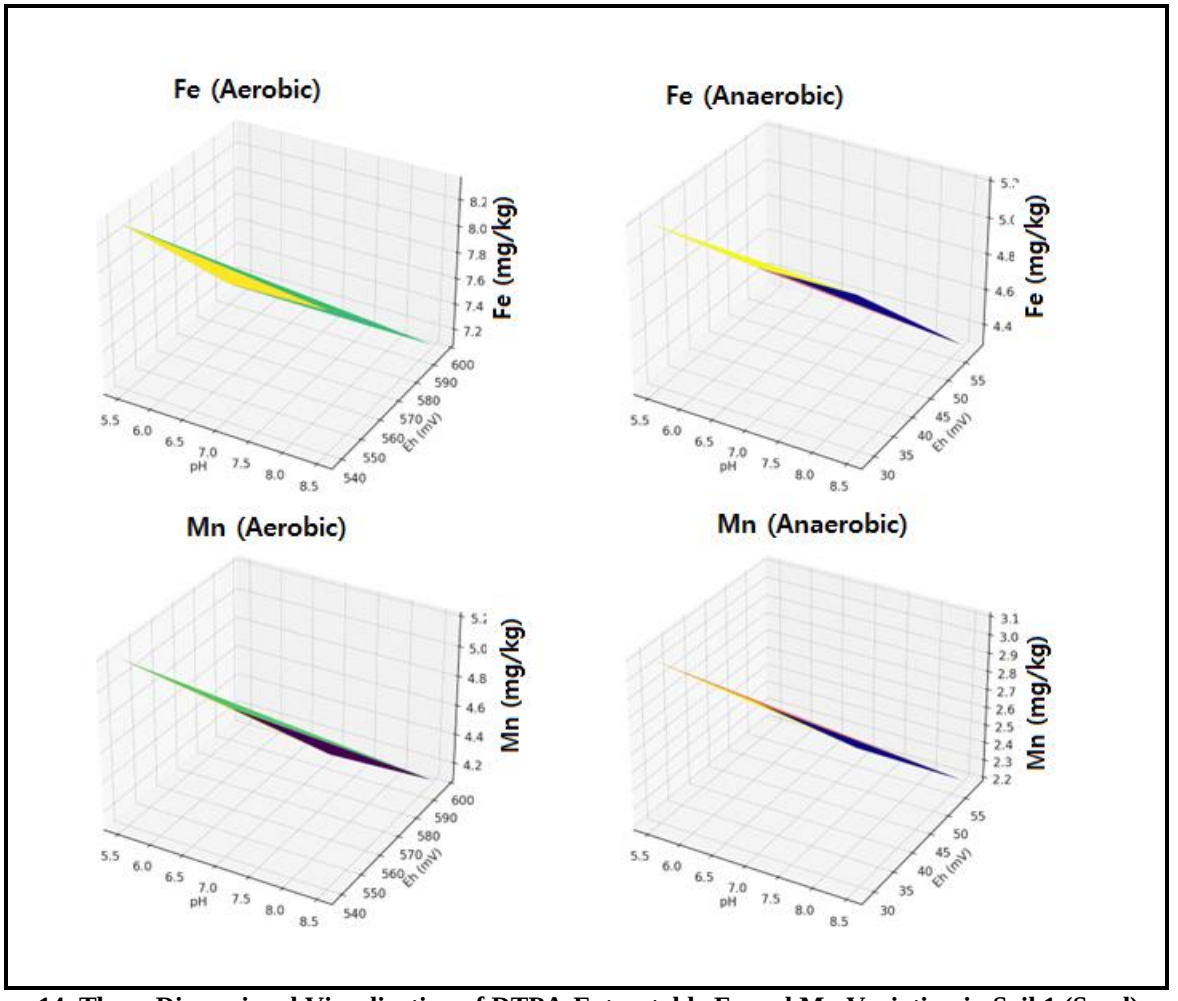

Figure 14. Three-Dimensional Visualization of DTPA-Extractable Fe and Mn Variation in Soil 1 (Sand) across Target pH Levels under Aerobic and Anaerobic Conditions during a 10-Day Laboratory Incubation

Table 15. DTPA-Extractable Iron (Fe) and Manganese (Mn) in Soil 7 (Clay) under Aerobic and Anaerobic Conditions at Different Target pH Levels during a 10-Day Laboratory Incubation

Treatment	Fe Mean ± SE	Mn Mean ± SE	Fe $LSD_{0.05}$	Mn $LSD_{0.05}$
pH 5.5 Aerobic	8.34 ± 0.02	5.20 ± 0.00	0.060	0.020
pH 5.5 Anaerobic	12.08 ± 0.02	8.10 ± 0.00	0.060	0.020
pH 6.5 Aerobic	6.66 ± 0.01	4.10 ± 0.00	0.030	0.015
pH 6.5 Anaerobic	9.88 ± 0.01	6.40 ± 0.00	0.030	0.015
pH 7.5 Aerobic	5.00 ± 0.00	3.10 ± 0.00	0.015	0.015
pH 7.5 Anaerobic	7.26 ± 0.01	4.90 ± 0.00	0.030	0.015
pH 8.5 Aerobic	3.34 ± 0.01	2.40 ± 0.00	0.030	0.015
pH 8.5 Anaerobic	4.80 ± 0.00	3.50 ± 0.00	0.015	0.015
Control Aerobic	2.90 ± 0.00	2.00 ± 0.00	0.015	0.015
Control Anaerobic	3.60 ± 0.00	2.80 ± 0.00	0.015	0.015

Note: Values represent means ± standard error (SE) of DTPA-extractable Fe and Mn concentrations ($mg \cdot kg^{-1}$) measured over the 10-day incubation period (n = 3). $LSD_{0.05}$ denotes the least significant difference at the 5% probability level for comparisons within each parameter, calculated from the standard errors and sample size.

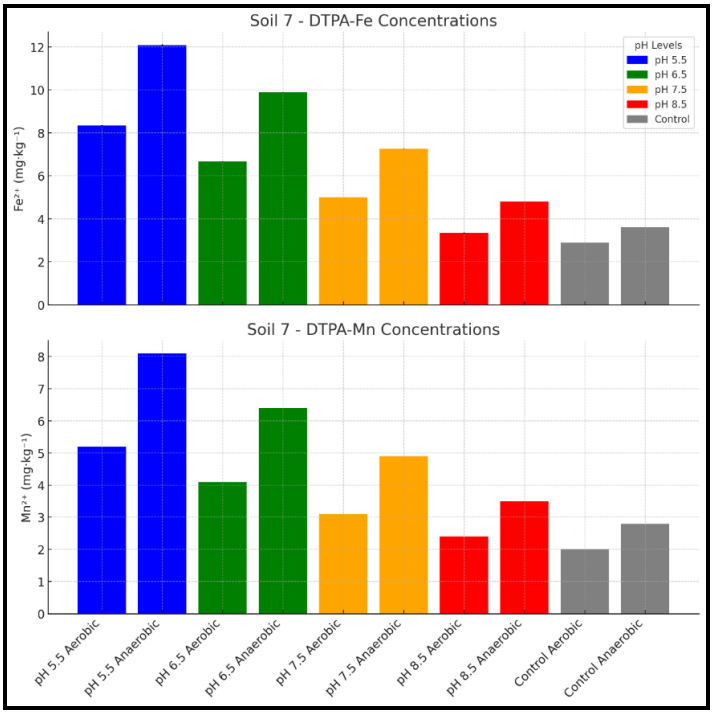

Figure 15. DTPA-Extractable Iron (Fe) and Manganese (Mn) in Soil 7 (Clay) under Aerobic and Anaerobic Conditions at Different Target pH Levels during a 10-Day Laboratory Incubation

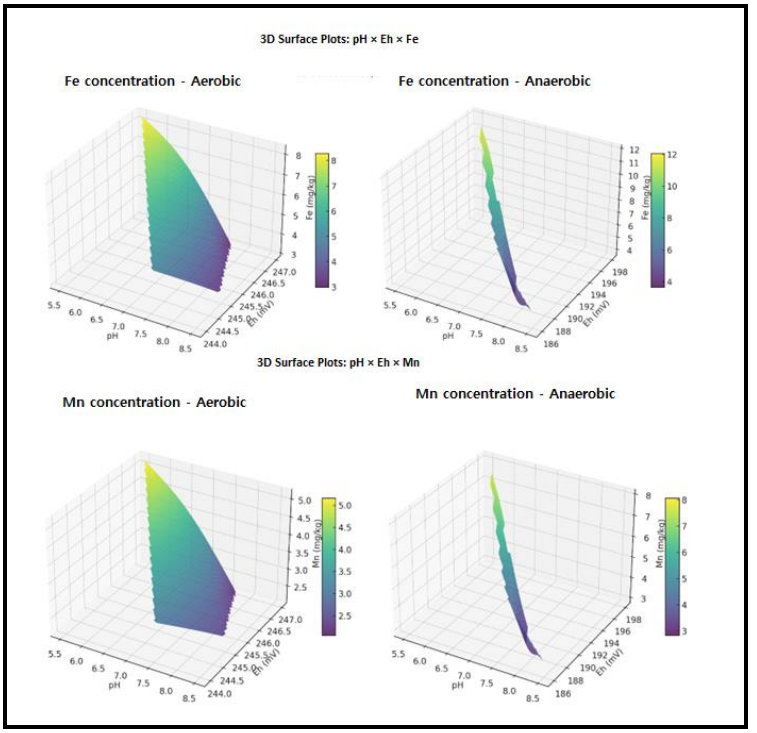

Figure 16. Three-Dimensional Visualization of DTPA-Extractable Fe and Mn Variation in Soil 7 (Clay) across Target pH Levels under Aerobic and Anaerobic Conditions during a 10-Day Laboratory Incubation

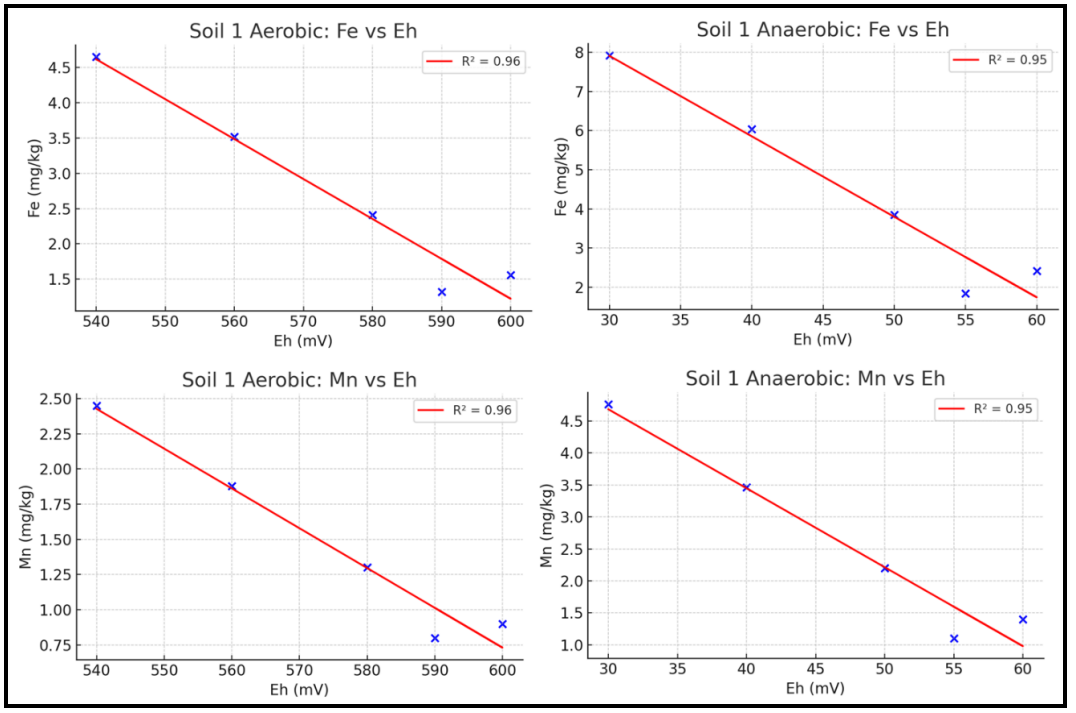

Figure 17. Coefficient of Determination (R^2) between Redox Potential (Eh) and DTPA-Extractable Fe and Mn in Soil 1 (Sand) under Aerobic and Anaerobic Conditions

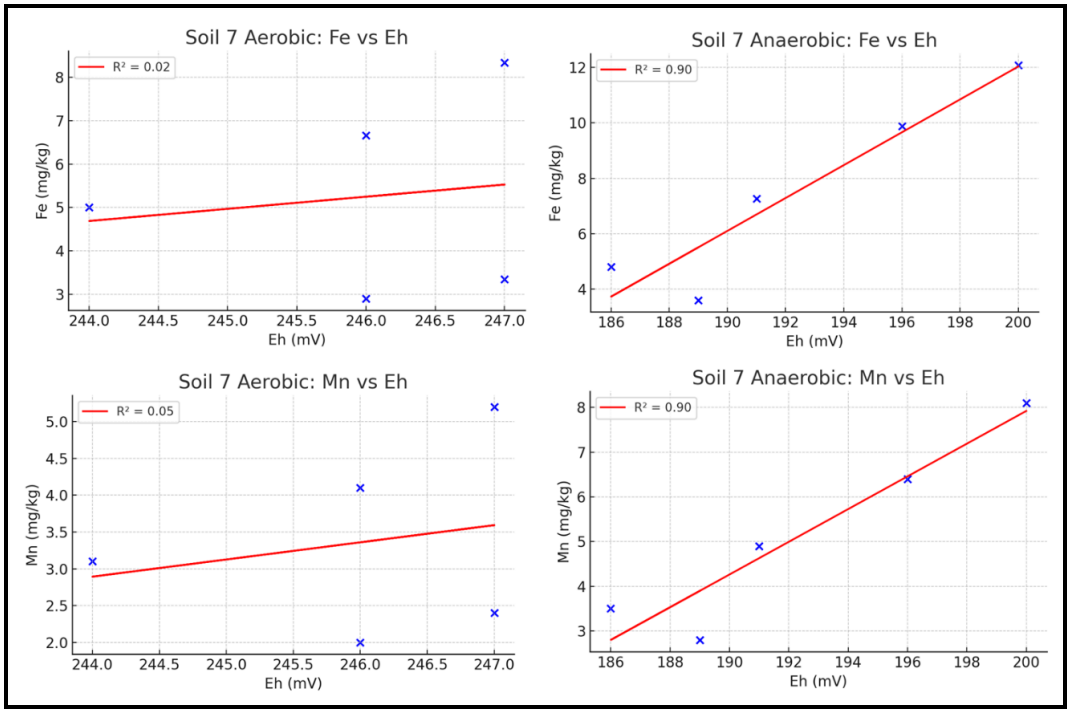

Figure 18. Coefficient of Determination (R^2) between Redox Potential (Eh) and DTPA-Extractable Fe and Mn in Soil 7 (Clay) under Aerobic and Anaerobic Conditions

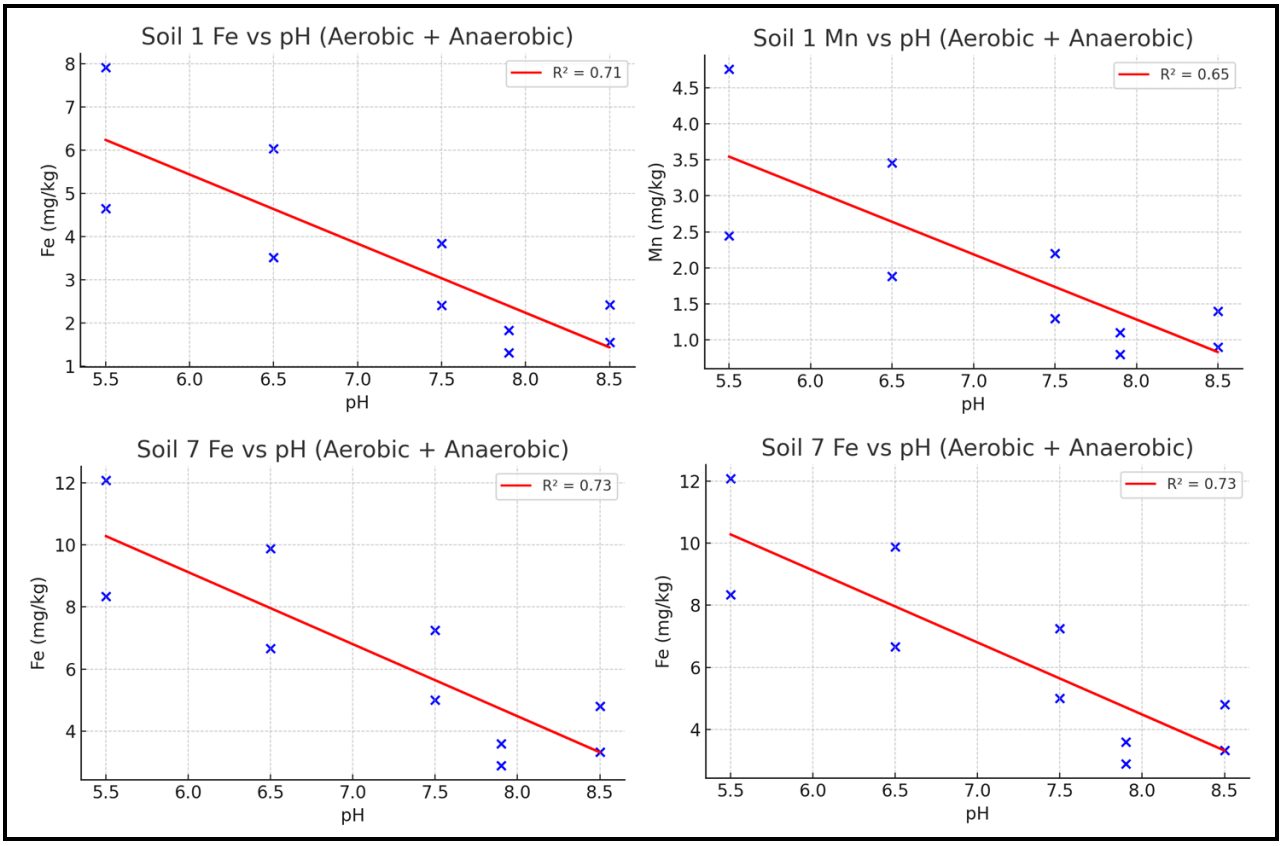

Figure 19. Coefficient of Determination (R^2) between Target pH and DTPA-Extractable Fe and Mn in Soil 1 (Sand) and Soil 7 (Clay) under Aerobic and Anaerobic Conditions

Table 16. Summary of Key Results for Soil 1 (Sand) and Soil 7 (Clay) from the 10-Day Laboratory Incubation

Parameter	Soil 1 ($mg \cdot kg^{-1}$)	Soil 7 ($mg \cdot kg^{-1}$)
Highest Fe^{2+} value	7.92 ± 0.01 (pH 5.5 Anaerobic)	12.08 ± 0.02 (pH 5.5 Anaerobic)
Lowest Fe^{2+} value	1.32 ± 0.00 (Control Aerobic)	2.90 ± 0.00 (Control Aerobic)
Relative Fe^{2+} increase from control (max)	≈ 6.0 times increase	≈ 4.2 times increase
Highest Mn^{2+} value	4.76 ± 0.01 (pH 5.5 Anaerobic)	8.10 ± 0.00 (pH 5.5 Anaerobic)
Lowest Mn^{2+} value	0.80 ± 0.00 (Control Aerobic)	2.00 ± 0.00 (Control Aerobic)
Relative Mn^{2+} increase from control (max)	≈ 5.95 times increase	≈ 4.05 times increase

Note: Summary of maximum and minimum values of DTPA-extractable Fe^{2+} and Mn^{2+}, relative increases from control treatments, and corresponding pH and redox conditions for each soil. Values are means ± standard error (SE).

Table 17. Rankings of Redox Buffer Capacity (RBC) for Soil 1 (Sand) and Soil 7 (Clay) under Different pH and Redox Conditions during a 10-Day Laboratory Incubation

Treatment	Soil 1 RBC (mV/day)	Soil 7 RBC (mV/day)
Highest RBC	0.11 (pH 5.5 Aerobic, Control Anaerobic)	0.56 (pH 8.5 Aerobic)
Lowest RBC	-0.22 (pH 7.5 Anaerobic)	-0.22 (pH 7.5 Anaerobic)
Notable Positive RBC	0 (Several treatments)	0.22 (pH 6.5 & 7.5 Aerobic)

Note: Highest and lowest RBC values and notable positive RBC values are summarized for each soil type. RBC values are expressed as the rate of change in redox potential ($mV\ day^{-1}$).

Table 18. Rankings of pH Buffer Capacity (pHBC) for Soil 1 (Sand) and Soil 7 (Clay) under Different pH and Redox Conditions during a 10-Day Laboratory Incubation

Treatment	Soil 1 pHBC (pH unit/day)	Soil 7 pHBC (pH unit/day)
Highest pHBC	0.0022 (pH 7.5 Anaerobic)	0.0022 (pH 7.5 Anaerobic)
Lowest pHBC	0 (Multiple treatments)	-0.0011 (pH 8.5 Aerobic)
Majority	Near zero	Near zero

Note: Highest and lowest pHBC values and general trends are summarized for each soil type. pHBC values are expressed as pH units per day.

5. Integrated Controls of Fe and Mn Availability in Calcareous and Reclaimed Soils

Results across field monitoring, laboratory incubations, and multivariate models points to three primary controls:

1. **Alkalinity and salinity set a low baseline** for Fe/Mn solubility (high pH, active $CaCO_3$, elevated EC).
2. **Soil attributes (texture, OM, CEC)** affect O_2 diffusion and ligand supply, thereby controlling reductive dissolution and chelation.
3. **Irrigation pulses impose brief reducing conditions** that transiently elevate DTPA-Fe and DTPA-Mn (Table 6B; Table 7).

Conceptual model. Multivariate response surfaces and path analysis indicate a two-tier regulation of Fe/Mn availability. At the base tier, alkaline pH and reactive $CaCO_3$ depress solubility, and elevated EC further constrains uptake (Grattan & Grieve, 1999 and Sparks *et al.,* 2023). Superimposed on this baseline, wetting-driven drops in O_2 and rises in CO_2—most pronounced in soils with higher OM and CEC—create micro-reducing niches and increase ligand supply, transiently elevating DTPA-Fe and DTPA-Mn. This framework reconciles the "total vs available" contrast and seasonal behavior: total Fe/Mn are largely soil-type constants, whereas DTPA-extractable pools are dynamic and track plant nutrition.

Seasonal dynamics. Correlation/regression results (Table 7) show DTPA-Fe/Mn negatively associated with pH, EC, and $CaCO_3$, and positively associated with moisture, CO_2, and OM (and inversely with O_2). The full models explain $R^2 \approx 0.93$ (Fe) and 0.91 (Mn), clarifying why post-irrigation wetting shifts DTPA values even when totals do not. Immediately after irrigation, moisture and CO_2 rise while O_2 falls, generating suboxic/anoxic microsites; DTPA-Fe/Mn increase accordingly. Because O_2 and CO_2 respond on hourly–daily scales, they delineate mobilization windows more reliably than spot Pt–Eh readings, which integrate multiple redox couples and can drift.

Laboratory validation. Incubations that hold pH (5.5–8.5) constant and switch only electron-acceptor status corroborate the causal ordering: Eh shifts under aerobic ↔ anaerobic far exceed those from pH adjustments alone, and the magnitude differs with texture-controlled gas diffusion and water retention, matching seasonal O_2/CO_2 patterns.

Management implications are clear:

- Apply **Fe(III)-EDDHA** under fertigation or soil application for persistent Fe deficiency, and foliar Mn ($MnSO_4$ or Mn-EDTA) when symptoms arise.
- Manage **salinity and irrigation** to keep EC low and exploit short-term reducing pulses without prolonged anoxia.
- Improve **OM and CEC** with compost/humics to stabilize mobilized Fe^{2+}/Mn^{2+}.
- **Time applications** near post-irrigation windows when mobilization peaks.
- **Monitor O_2/CO_2 and DTPA-Fe/Mn**, which are more reliable than isolated Pt–Eh readings.

CONCLUSION

This study demonstrated that the solubility and bioavailability of Fe and Mn in the calcareous soils of the Farafra Oasis are governed by the interplay of carbonate alkalinity and redox–pH dynamics.The solubility and availability of iron (Fe) and manganese (Mn) in the calcareous soils of the Farafra Oasis are primarily controlled by carbonate alkalinity and redox-pH dynamics. Total Fe and Mn concentrations are not good indicators of plant availability.

- **Factors Increasing Availability:** Finer-textured soils rich in clay and organic matter (OM) have a higher cation exchange capacity (CEC) and lower redox potential, promoting the dissolution of Fe and Mn into plant-available forms (Fe^{2+} and Mn^{2+}). Short-term irrigation also temporarily boosts Fe and Mn availability by creating reducing conditions.
- **Factors Decreasing Availability:** Coarse-textured, carbonate-rich soils have high pH and redox potential (Eh), severely limiting the availability of these micronutrients. High pH and calcium carbonate ($CaCO_3$) buffering consistently suppress soluble Fe and Mn.

- **Management Implications:** To improve crop productivity, an integrated approach is needed.

A. Additions: Use organic matter like compost to promote chelation and create reducing conditions.

B. Fe Deficiency: Apply Fe-EDDHA, which is stable at high pH.

C. Mn Deficiency: Use foliar sprays of $MnSO_4$ or Mn-EDTA.

D. Irrigation: Optimize irrigation to maintain soil moisture without causing prolonged waterlogging.

In essence, Fe and Mn nutrition in these soils is limited by their dynamic partitioning between insoluble and bioavailable pools, a process governed by alkalinity, salinity, redox buffering, and organic matter.

REFERENCES

Abrol, I. P., J. S. P. Yadav and F. I. Massoud. 1988. Salt-affected soils and their management (FAO Soils Bulletin No. 39). Food and Agriculture Organization of the United Nations, Rome.

Alejandro, S., S. Höller, B. Meier, and E. Peiter. 2020. Manganese in plants: From acquisition to subcellular allocation. Frontiers in Plant Science, 11, 300. https://doi.org/10.3389/fpls.2020.00300

Alloway, B. J. 2019. Soil factors associated with zinc deficiency in crops and humans. *Environmental Geochemistry and Health, 41*(6): 2231–2249. https://doi.org/10.1007/s10653-019-00270-9

Cornell, R. M., and U. Schwertmann. 2003. The Iron Oxides: Structure, Properties, Reactions, Occurrences and Uses (2nd ed.). Wiley-VCH. https://doi.org/10.1002/3527602097

de Santiago, A., J. M. Quintero and A. Delgado. 2008. Long-term effects of tillage on the availability of iron, copper, manganese, and zinc in a Spanish Vertisol. *Soil and Tillage Research, 98*(1):200–207. https://doi.org/10.1016/j.still.2008.01.002

Dhaliwal, S. S., V. Sharma, A. K. Shukla, V. Verma, M. Kaur, A. M. Alsuhaibani, A. Gaber, P. Singh, A. M. Laing and A. Hossain. 2023. Minerals and chelated-based manganese fertilization influence the productivity, uptake, and mobilization of manganese in wheat (*Triticum aestivum* L.) in sandy loam soils. *Frontiers in Plant Science, 14*, Article 1163528. https://doi.org/10.3389/fpls.2023.1163528

El-Sherif, A. G., M. G. Abd El-Kader, B. A. El-Haddad, and M. S. Abo El-Kheir. 2018. Characterization and classification of soils in Farafra Oasis, Western Desert, Egypt. Egyptian Journal of Soil Science, 58(2), 133–148. https://doi.org/10.21608/ejss.2018.3240.1126

Evans, A. E., M. A. Limmer and A. L. Seyfferth. 2021. IRIS films as a water-management tool for rice farmers. *Journal of Environmental Management, 294*, 112920. https://doi.org/10.1016/j.jenvman.2021.112920

Fadl, M. E., A. S. Abuzaid, M. A. E. AbdelRahman and A. Biswas. 2022. Evaluation of desertification severity in El-Farafra Oasis, Western Desert of Egypt: Application of modified MEDALUS approach using wind erosion index and factor analysis. *Land*, 11(1). 54. https://doi.org/10.3390/land11010054

Fiedler, S., M. J. Vepraskas, and J. L. Richardson. 2007. Soil redox potential: Importance, field measurements, and observations. Advances in Agronomy, 94, 1–54. https://doi.org/10.1016/S0065-2113(06)94001-2

Gomez, K. A., and A. A. Gomez. 1984. Statistical Procedures for Agricultural Research (2nd ed.). New York: John Wiley & Sons.

Grattan, S. R. and C. M. Grieve. 1999. Salinity–mineral nutrient relations in horticultural crops. *Scientia Horticulturae, 78*(1–4):127–157. https://doi.org/10.1016/S0304-4238(98)00192-7.

Hodges, C., S. Fiedler, J. Rinklebe and M. Koschorreck. 2023. Using fixed-potential electrodes to quantify Fe and Mn redox cycling in upland soils. *Biogeochemistry, 162*(1):25–42. https://doi.org/10.1007/s10533-022-01012-9.

Ismail, H. A., S. M. El-Marsafawy, and A. I. El-Morsy. 2016. Soil properties and land capability assessment in Farafra Oasis, Western Desert, Egypt. Journal of Soil Sciences and Agricultural Engineering, 7(2), 117–130. https://doi.org/10.21608/jssae.2016.35458

Jien, S.-H. and C.-S. Wang. 2019. Effects of different clay minerals on soil hydraulic properties: Capillary retention, water-holding capacity, and infiltration. *Journal of Soil Science and Plant Nutrition, 19*(2):345–358. https://doi.org/10.1007/s42729-019-00001-0

Klopp, H. W., F. J. Arriaga and W. F. Bleam. 2020. *Influence of exchangeable sodium and clay mineralogy on soil water retention and hydraulic conductivity*. Journal of Soil and Water Conservation, 75(6): 755–764. https://doi.org/10.2489/jswc.2020.00182

Klute, A. 1986. Water retention: Laboratory methods. In A. Klute (Ed.), Methods of Soil Analysis. Part 1—Physical and Mineralogical Methods (2nd ed., pp. 635–662). Madison, WI: ASA and SSSA. https://doi.org/10.2136/sssabookser5.1.2ed.c26

Lakshani, M. M. T., J. R. R. N. Jayarathne, K. Kawamoto, T. S. Komatsu and P. Moldrup. 2023. A new exponential model for predicting soil gas diffusivity with varying degree of saturation. *Vadose Zone Journal*, *22*(1), e20236. https://doi.org/10.1002/vzj2.20236

Lakshani, M. M. T., J. R. R. N. Jayarathne, K. Kawamoto, T. S. Komatsu, and P. Moldrup. 2023. A new exponential model for predicting soil gas diffusivity with varying degree of saturation. Vadose Zone Journal, 22(1), e20236. https://doi.org/10.1002/vzj2.20236

Lindsay, W. L. and W. A. Norvell. 1978.Development of a DTPA soil test for zinc, iron, manganese, and copper. *Soil Science Society of America Journal*, *42*(3): 421–428. https://doi.org/10.2136/sssaj1978.03615995004200030009x

López-Rayo, S., P. Nadal and J. J. Lucena. 2015. Novel chelating agents for iron, manganese, zinc, and copper mixed fertilisation in high pH soilless cultures. *Journal of the Science of Food and Agriculture*, *95*(11): 2270–2276. https://doi.org/10.1002/jsfa.7183

Lovley, D. R. 1991. Dissimilatory Fe(III)- and Mn(IV)-reducing prokaryotes. In A. Balows, H. G. Trüper, M. Dworkin, W. Harder, and K.-H. Schleifer (Eds.), The Prokaryotes (pp. 635–658). Springer. https://doi.org/10.1007/0-387-30742-7_21

Montgomery, D. C. 2017. Design and Analysis of Experiments (9th ed.). Hoboken, NJ: John Wiley & Sons.

Najafi-Ghiri, M., N. Karimian and H. Arzani. 2010. Factors affecting micronutrient availability in calcareous soils of southern Iran. *Geoderma*, *158*(3–4):150–156. https://doi.org/10.1016/j.geoderma.2010.04.009

Palansooriya, K. N., Y. Yang, Y. F. Tsang, B. Sarkar, D. Hou, X. Cao, E. Meers, J. Rinklebe, K.-H. Kim, and Y. S. Ok. 2020. Occurrence of contaminants in drinking water sources and the potential of biochar for water quality improvement: A review. Critical Reviews in Environmental Science and Technology, 50(6), 549–611. https://doi.org/10.1080/10643389.2019.1629803

Palihakkara, N. L., M. J. Vepraskas, and D. L. Lindbo. 2016. Redox potentials and reduction–oxidation processes in soils: Implications for soil color and hydric soil indicators. Journal of Environmental Quality, 45(4), 1173–1183. https://doi.org/10.2134/jeq2015.11.0547

Patrick, W. H., and R. D. DeLaune. 1973. Formation of redox potential in waterlogged soils and its relation to the release of elements. Soil Science Society of America Proceedings, 37(3), 331–337. https://doi.org/10.2136/sssaj1973.03615995003700030010x

Ponnamperuma, F. N. 1972. The chemistry of submerged soils. Advances in Agronomy, 24, 29–96. https://doi.org/10.1016/S0065-2113(08)60633-1

Rai, S., P. K. Singh, and S. Mankotia. 2021. Iron homeostasis in plants and its crosstalk with copper, zinc, and manganese. Plant Stress, 1, 100008. https://doi.org/10.1016/j.stress.2021.100008

Rajput, R. S., A.Singh and M. K. Mishra. 2023. Hydroxide precipitation of complexed metals. *Reviews in Environmental Science and Bio/Technology*, *22*(1):189–210. https://doi.org/10.1007/s11157-022-09642-8

Reddy, K. R. and R. D. DeLaune. 2008. *Biogeochemistry of Wetlands: Science and Applications* (1st ed.). Boca Raton, FL: CRC Press. https://doi.org/10.1201/9780203491454

Rietz, D. N. and R. J. Haynes. 2003. Effects of irrigation-induced salinity and sodicity on soil microbial activity. activity. *Soil Biology & Biochemistry*, *35*(6):, 845–854. https://doi.org/10.1016/S0038-0717(03)00125-1

Rojas, C. L., F. J. Romera, E. Alcántara, R. Pérez-Vicente, C. Sariego, J. I. García-Alonso, J. Boned and G. Martí. 2008. Efficacy of Fe (o,o-EDDHA) and Fe (o,p-EDDHA) isomers in supplying Fe to Strategy I plants differs in nutrient solution and calcareous soil. *Journal of Agricultural and Food Chemistry*, *56*(22):10774–10778. https://doi.org/10.1021/jf8022589

Sander, M., and M. Koschorreck. 2020. Redox potential measurements: Perspectives and limitations for real-time environmental monitoring. Environmental Science & Technology, 54(2), 1098–1107. https://doi.org/10.1021/acs.est.9b05590

Shakeria, S. and M. Saffari. 2020. The status of chemical forms of iron and manganese in various orders of calcareous soils and their relationship with some physicochemical and mineralogical properties. *Communications in Soil Science and Plant Analysis*, *51*(15):2054–2068. https://doi.org/10.1080/00103624.2020.1820026

Sharma, A., A. K. Nagpal and B. Singh. 2017. Influence of redox potential on iron and manganese transformation in soils: A review. *Pedosphere*, *27*(3);407–420. https://doi.org/10.1016/S1002-0160(17)60338-4

Sharma, S. S., V. Singh, J. Kumar, A. K. Singh and V. K. Singh. 2022. The pedospheric variation of DTPA-extractable Zn, Fe, Mn, Cu and other micronutrients in different soil orders. *Sustainability*, *14*(1); 29. https://doi.org/10.3390/su14010029

Smythers, A. L., J. R. Crislip, D. R. Slone, B. B. Flinn, J. E. Chaffins, K. A. Camp, E. W. McFeeley, and D. R. J. Kolling. 2023. Excess manganese increases photosynthetic activity via enhanced reducing center and antenna plasticity in Chlorella vulgaris. Scientific Reports, 13, 11301. https://doi.org/10.1038/s41598-023-35895-x

Sparks, D. L. 2003. *Environmental soil chemistry* (2nd ed.). San Diego, CA: Academic Press. https://doi.org/10.1016/B978-0-12-656446-4.X5000-9

Sparks, D. L. 2003. Environmental soil chemistry (2nd ed.). San Diego, CA: Academic Press. https://doi.org/10.1016/B978-0-12-656446-4.X5000-9

Sparks, D. L. 2023. Environmental Soil Chemistry (3rd ed.). Cambridge, MA: Academic Press (Elsevier).

Totsche, K. U., W. Amelung, M. H.Gerzabek, G. Guggenberger, E. Klumpp, C. Knief, E. Lehndorff, R. Mikutta, S. Peth, A. Prechtel, N. Ray and I. Kögel-Knabner. 2018. Microaggregates in soils. *Journal of Plant Nutrition and Soil Science*, *181*(1):104–136. https://doi.org/10.1002/jpln.201600451

Valdés-Abellán, J. 2024. Estimating the universal scaling of gas diffusion in coarse-textured soils. *Geoderma*, *438*, 116900. https://doi.org/10.1016/j.geoderma.2023.116900

Violante, A., M. Pigna and L. Gianfreda. 2010. Mobility and bioavailability of heavy metals and metalloids in soil environments. *Journal of Soil Science and Plant Nutrition*, *10*(3): 268–292. https://doi.org/10.4067/S0718-27912010000100005

Wu, C., Y. Dun, Z. Zhang, M. Li, G. Wu and X. Xu. 2021. Forms and availability of micronutrients in soils as affected by land uses and soil types in the red soil region of China. *Journal of Soils and Sediments*, *21*(2): 747–760. https://doi.org/10.1007/s11368-020-02799-w

Yassin, S. A., S. Y. Awadalla, E. M. El-Hadidi, M. M. Ibrahim, and A. A. Taha. 2023. Assessment of the compost addition and sandification to overcome the calcium carbonate problems in heavy clay calcareous soils at El Farafra Oasis – Egypt. Egyptian Journal of Soil Science, 63(3), 311–323. https://doi.org/10.21608/ejss.2023.212242.1596

Yin, M., H. Xiao, C. Liu and T. Liu. 2020. Distribution, speciation and availability of soil micronutrients as affected by land use in a long-term field experiment. *Catena*, *194*. 104725. https://doi.org/10.1016/j.catena.2020.104725

Yu, K. W., S. P. Faulkner, and W. H. Patrick. 2001. Redox potential characterization and soil reduction in a coastal forest. Soil Science Society of America Journal, 65(5), 1518–1527. https://doi.org/10.2136/sssaj2001.6551518x

Zubieta, A. S., L. R. Geiss, E. R. C. Espinosa and E. G. Matcham. 2025. Manganese foliar fertilizer does not impact yield or grade of Florida peanut. *Agrosystems, Geosciences & Environment*, *8*, e70058. https://doi.org/10.1002/agg2.70058

الملخص العربي

التأثيرات المتداخة بين جهد الأكسدة والإختزال ورقم تفاعل التربة على ذوبان الحديد والمنجنيز فى أراضى واحة الفرافرة، مصر

سحر محمد إسماعيل

تعد نقص العناصر الصغرى، وخاصة الحديد (Fe) والمنجنيز (Mn)، من أهم القيود التي تحد من إنتاجية المحاصيل في الأراضي الجيرية بالمناطق الجافة وشبه الجافة. وتتميز واحة الفرافرة بمصر، بقوام خشن، وارتفاع محتوى كربونات الكالسيوم ($CaCO_3$)، وانخفاض المادة العضوية، وارتفاع درجة التفاعل (pH) القلوية—وهي ظروف تحد من ذوبان الحديد والمنجنيز على الرغم من وفرة مخزونهما الكلي. تهدف هذه الدراسة إلى توضيح التأثيرات التفاعلية المتداخلة لجهد الأكسدة والاختزال (Eh)، ودرجة تفاعل التربة (pH)، والقدرة التنظيمية للكربونات، والخصائص الفيزيوكيميائية للتربة على ذوبان وتوافر الحديد والمنجنيز تحت الظروف الحقلية والمعملية. تم توصيف سبعة أنواع من الأراضى، تتراوح من الرملية إلى الطينية، باستخدام حيود الأشعة السينية (XRD)، (XRF)، وتحليلات كيميائية تفصيلية. كما جرى رصد موسمي حقلى تحت زراعة الذرة الرفيعة لتقييم Eh، وpH، والرطوبة، وتركيز O_2 وCO_2، والحديد والمنجنيز المستخلص بـ DTPA عبر دورات الري. كذلك أُجريت تجربة تحضين لتربة رملية وأخرى طينية لتقييم القدرات التنظيمية لجهد الأكسدة والإختزال (RBC) ودرجة تفاعل التربة (pHBC) تحت ظروف هوائية ولاهوائية. أظهرت النتائج أن الحديد الكلي (١٤،٨٠٠–٢٠،٢٠٠ ملجم/كجم) والمنجنيز الكلي (٢٨٠–٨٢٠ ملجم/كجم) لم يكونا مؤشرات دقيقة لتيسرهما للنبات، إذ بقيت الصور المستخلصة بـ DTPA أقل من ٠.٠٣٪ من الإجمالي. سجلت التربة الرملية (تربة ١) أقل قيم للصور المستخلصة من الحديد (4.5 ملجم/كجم)، 3.0ملجم/كجم من المنجنيز، بينما سجلت التربة الطينية الغنية بالمادة العضوية نسبيا (تربة ٧) أعلى القيم من الحديد (٦.٥ ملجم/كجم)، 6.2 ملجم/كجم من المنجنيز. ارتبطت تركيزات الحديد والمنجنيز المستخلصة سلبياً مع pH والتوصيل الكهربائى للأملاح (EC) و الكرونات الكلية ($CaCO_3$)، وإيجابياً مع المادة العضوية (OM) والسعة التبادلية الكاتيونية (CEC) والرطوبة وتدفّق ثانى أكسيد الكربون (CO_2). أظهرت نماذج الارتباط والانحدار أن معامل الإنحدار (R^2) بلغ 0.93 للحديد و 0.91 للمنجنيز، مما يدل على أن أكثر من ٩٠٪ من التباين في توافر الحديد والمنجنيز يمكن تفسيره بخصائص التربة الفيزيوكيميائية والظروف الحقلية المدروسة. وأكدت تجربة التحضين المعملية أن نظام الأكسدة–الاختزال هو العامل الأكثر تحكماً في Eh مقارنةً بـ pH. توضح هذه النتائج أن توافر الحديد والمنجنيز لا يعتمد على محتواهما الكلي بل على التفاعلات الديناميكية بين القلوية وتركيز الأملاح والقدرة التنظيمية للأكسدة والإختزال والمادة العضوية. ويوصى باستخدام إستراتيجيات متكاملة—تشمل إضافة محسنات عضوية، وتسميد بالـ-Fe EDDHA، ورش ورقى للمنجنيز، وجدولة الري—لضمان استدامة إنتاجية المحاصيل في الأراضي الصحراوية المستصلحة.

الكلمات المفتاحية: الأراضى الجيرية، جهد الأكسدة والإختزال، رقم تفاعل التربة، ذوبان الحديد والمنجنيز، واحة الفرافرة ، إدارة العناصر الصغرى.